DOI: 10.1002/ejoc.200901234

Chemoselective Reagents for Covalent Capture and Display of Glycans in Microarrays

Emiliano Cló,[a] Ola Blixt,[b] and Knud J. Jensen*[a,c]

Dedicated to Professor Klaus Bock on the occasion of his 65th birthday

Keywords: Nanobioscience / Glycomics / Microarrays / Lectins / Carbohydrates / Chemoselectivity

Glycobiology has made very significant progress in the past decades. However, further progress will significantly depend on the establishment of novel methods for miniaturized, high-throughput analysis of glycan–protein interactions. Robust solid-phase chemical tools and new, chemoselective reagents for biologically meaningful display of surface-immobilized glycans are likely to play a key role. Here we present four new bifunctional linkers that allow highly chemoselective capture of unprotected glycans in solution to form glycan-linker conjugates for direct construction of glycan microarrays (glycochips). The bifunctional linkers carry *O*-linked aminooxy moieties, some with *N*-substituents at one end and an amino group at the other. In addition, they contain a substituted benzene ring for UV traceability and improved purification of glycan-linker conjugates. NMR spectroscopic studies in solution proved that *N*-substituted aminooxy linkers provided model glycan-linker conjugates with the β-glucopyranoside configuration, i.e. the ring-closed form required for biological recognition. Then an ensemble of glycan-linker conjugates were assembled from mannobiose, lactose, and *N*-acetyl-lactosamine and used for covalent printing of glycan microarrays. The stability of oximes were studied both in solution and on-chip. In solution, two of the linkers provided glycan-linker conjugates with a remarkable stability at pH 4 or higher, on-chip this relative stability was upheld. Two of the linkers, with different properties, are recommended for the glycobiology toolbox for the construction of glycan microarrays from unprotected glycans.

Introduction

In the post-genomic era the study of glycobiology has attracted considerable attention, as most proteins in living systems require post-translational modifications, most commonly glycosylation, for correct function.[1] Glycans are essential for life processes, including intra- and inter-cellular signaling,[2] host-guest interaction,[3] cell adhesion,[4] fertilization[5] and tumor proliferation.[6] The term "glycomics" covers the comprehensive study of all glycan structures of a given cell type or organism.[7] The absence of an apparent direct flow of information from the genome to the glycome, combined with the pronounced structural complexity of the primary structure of glycans, makes the study of the glycome extremely complex. To facilitate the functional mapping of the glycome, new techniques that allow for a high-throughput screening of carbohydrate probes with several glycan-binding proteins (GBP) and glycan-processing enzymes (GPE) are important.

Recently, a composite set of solid-phase tools for glycobiology specially devised to support high-throughput screening has been emerging.[8] One of the most prominent of such tools is represented by glycan microarray technology,[9] in which a broad range of interaction types and materials have been used to anchor the glycan probes onto the solid support.[10] Ideally, glycan microarrays (i.e. glycochips) should be able to present the glycans in a biologically meaningful fashion. As GBPs typically require multivalency[11] for efficient binding, presentation of the probe structures should optimally occur in a clustered and directional fashion. Furthermore, it is desirable to present glycans isolated from naturally occurring specimens on glycochips. The attachment of glycans onto the array should use methodologies that allow it to be robust and spatially defined, such as covalent bonding. Several approaches to covalent glycochips have been described in recent years, in which different types of attachment chemistries were successfully applied, for example 1,3 dipolar cycloaddition between an azide and an alkyne,[12] amide bond formation,[13] epoxide opening,[14] Michael addition of thiols to malem-

[a] IGM, Faculty of Life Sciences, University of Copenhagen,
Thorvaldsensvej 40, 1871 Frederiksberg, Denmark
Fax: +45-3533-2398
E-mail: kjj@life.ku.dk
[b] Copenhagen Center for Glycomics, Department of Cellular and Molecular Medicine, Faculty of Health Sciences, University of Copenhagen,
Blegdamsvej 3, 2200 Copenhagen, Denmark
[c] Centre for Carbohydrate Recognition and Signaling, University of Copenhagen,
Thorvaldsensvej 40, 1871 Frederiksberg, Denmark

Supporting information for this article is available on the WWW under http://dx.doi.org/10.1002/ejoc.200901234.

ides[15] and Staudinger ligation.[16] However, most protocols require the carbohydrate probes to be constructed through multi-step synthesis in order to fashion them with the spacer moiety able to react with the solid support of choice. This process is time consuming, requires specialized skills in synthetic carbohydrate chemistry and makes the utilization of glycans isolated from natural sources very difficult. Thus, the preparation of glycans for the glycochip is the bottleneck of the whole process, preventing covalent glycan microarrays from becoming a true high-throughput process.

An attractive option to bypass extensive organic synthesis for probe preparation is to make use of chemoselective reactions between the native underivatized glycans and a bifunctional linker. The presence of an aldehyde moiety at the reducing end of glycans can be used for chemoselective couplings with strong α-nucleophiles such as hydrazines, hydrazones, sulfonylhydrazides and hydroxylamines and several examples of these glycoconjugates have been described.[17] Some glycochips have already been designed to take advantage of these chemoselective couplings. For example, oligosaccharides have been chemoselectively coupled with aminooxy-type linkers in solution, and the linker allowed specific, non-covalent absorption onto the chip surface.[18] Alternatively, the manufacture of slide surfaces coated with a suitable functional linker type exposing the α-nucleophile to react with underivatized glycans spotted onto it has also been described. The groups of Shin[19] and Turnbull[20] have both applied this concept to the construction of hydrazide-coated microarrays starting from glass and gold as solid supports, respectively. Moreover, conjugation of free reducing oligosaccharides with a suitable spacer moiety by imine formation followed by in situ reductive amination has been pursued in recent years. Cummings and co-workers[21] reported a method to derivatize glycans with 2,6-diaminopyridine linker (DAP) in order to generate covalent microarrays onto NHS-activated glass slides. This approach greatly reduced the synthetic manipulations needed to access derivatized carbohydrates, yet it exclusively furnished open-chain structures of the core monosaccharides and had limited reactivity with the activated glass slide.

We reasoned that it would be desirable to develop a methodology for covalent glycan microarray fabrication that could avoid extensive synthetic efforts and allow for fast isolation of glycan-linker conjugates. The centerpiece of the linker design was the choice of α-nucleophile to provide stable conjugates and, ideally, retaining (at least partially) the cyclic nature of the sugar moiety at the reducing end. The thermodynamic stability of substitution products between aldehydes and α-nucleophiles is known to be the highest for hydroxylamine nucleophiles.[22] Also, *N*-alkyl-substituted hydroxylamines can direct the stereochemistry at the saccharide reducing unit towards the retention of the ring-closed pyranose structure (either exclusively, as with glucose, or predominantly, as with mannose and galactose).[23] The presentation of at least some of the glycan core structure in the ring-closed form has proven to be of crucial importance for functional recognition of glycans by GBP and GPE, especially when interrogating short-chain saccharides, as reported by Feizi et al. for neoglycolipids probes absorbed onto nitrocellulose microarrays[18a] and recently highlighted by Thygesen[24] et al. for gold nanoparticles. The only example available to date reporting the use of a chemoselective bifunctional linker allowing solution-phase glycan-linker coupling and subsequent covalent attachment onto a reactive slide was provided by Blixt and co-workers.[25] This simple linear aliphatic linker comprised both a *N*-methylhydroxylamine moiety, for chemoselective coupling with glycans, and a primary amine functionality suitable for the attachment onto *N*-hydroxysuccinimide (NHS)-activated glass slides. However, this valuable linker did not allow easy quantification of the glycoconjugates. In addition, precise information on the stability of glycan-linker conjugates constructed from α-nucleophiles is needed.

Here we present a panel of novel aminooxy-type bifunctional linkers bearing different N,O-substitution patterns. To the best of our knowledge, no direct comparison of structurally related aminooxy-type glycoconjugates, which include both primary and secondary, *N*-alkylhydroxylamines, is available to date for microarrays. Glycoconjugates with glucose as a model glycan were prepared in milli-

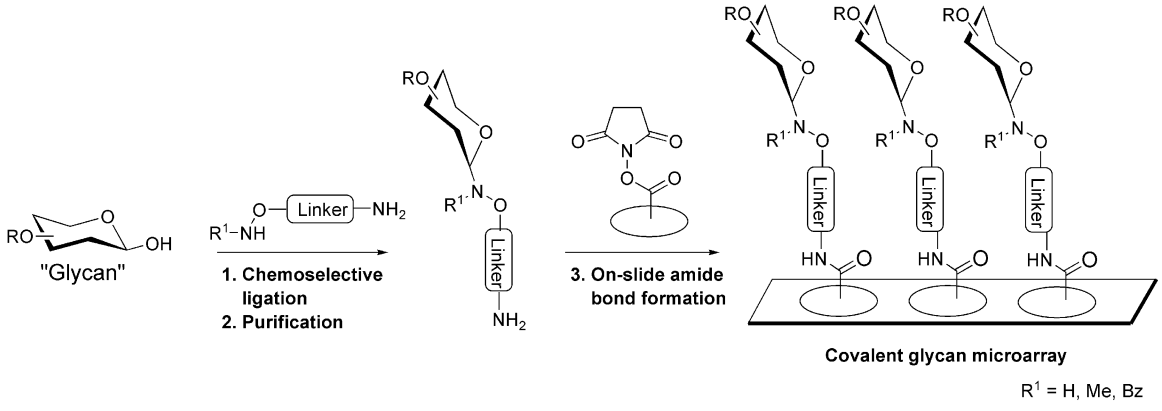

Scheme 1. Overview of three-step procedure involving glycan chemoselective coupling to the bifunctional linker, purification of the glycoconjugate and on-slide covalent fixation via amide bond formation.

gram amounts to assess both their stereochemistry and their hydrolytic stability. Furthermore, the applicability of a three-step scheme (i.e. coupling, purification and on-chip reaction) for the fabrication of glycan microarrays with common saccharides (Scheme 1) was tested and the performance of the different glycoconjugates with GBPs evaluated.

Results and Discussion

Preparation of Bifunctional Linkers and of Glucose-Linker Conjugates

Linker Synthesis: The five linkers addressed by the present study are presented in Figure 1; **M-AE** linker was originally developed by Blixt and co-workers[25] and was used as reference compound. The remaining four are novel structures which incorporate an aminooxy functionality for chemoselective glycan capture, a primary amino group for on-chip amide bond formation and an aromatic chromophore moiety for UV detection of the target conjugates during HPLC purification. The synthesis of *N*-benzylated *O*-alkylated hydroxylamine linker **B-AE** made use of *N*-benzylhydroxylamine as the central building block (Scheme 2, A). The nitrogen was first Boc-protected in order to react the hydroxy group with *N*-Boc-2-bromoethylamine in the presence of DBU as base in a microwave reactor at 65 °C for 40 min, thus furnishing the fully Boc-protected target linker **Boc(B-AE)** in 38% yield over two steps. Removal of the acid-labile Boc groups was performed with HCl in dioxane, which gave the desired **B-AE** linker in 74% yield. The use of acidic dioxane was preferred over neat trifluoroacetic acid as the product upon deprotection became insoluble in

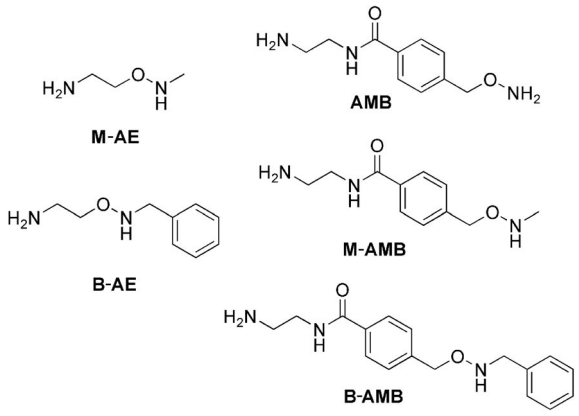

Figure 1. Target linkers: 2-(methylaminooxy)ethanamine (**M-AE**), 2-(benzylaminooxy)ethanamine (**B-AE**), *N*-(2-aminoethyl)-4-(aminooxymethyl)benzamide (**AMB**), *N*-(2-aminoethyl)-4-[(methylaminooxy)methyl]benzamide (**M-AMB**), *N*-(2-aminoethyl)-4-[(benzylaminooxy)methyl]benzamide (**B-AMB**).

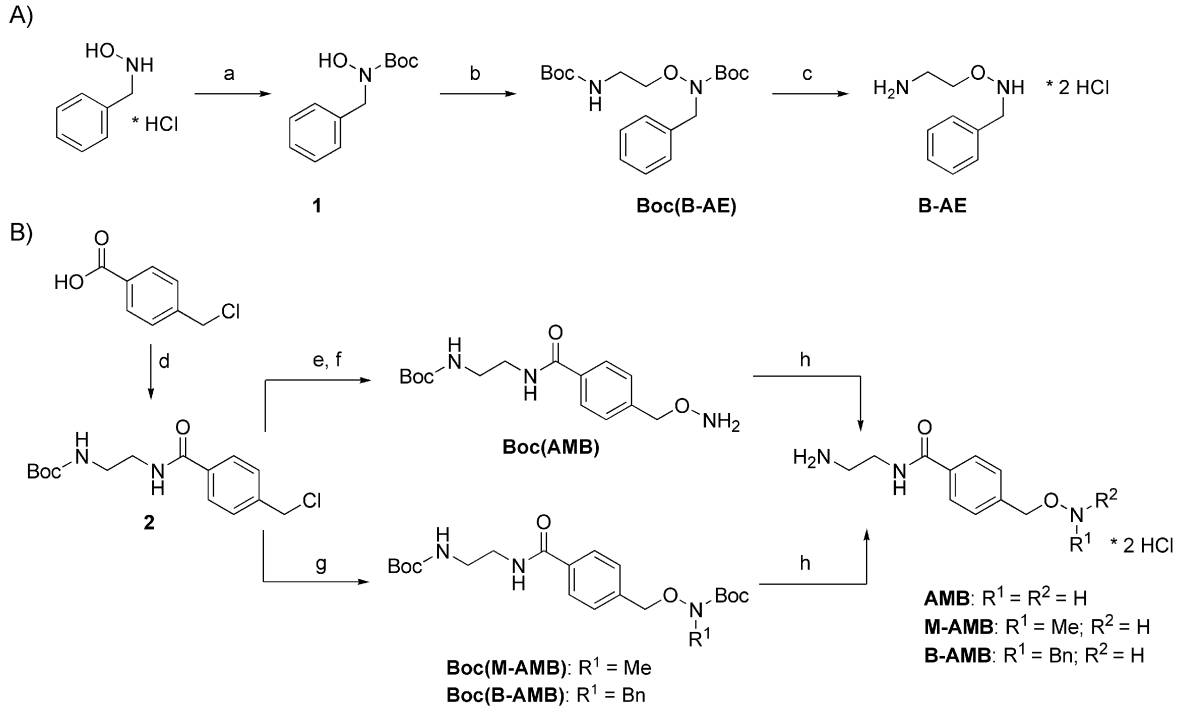

Scheme 2. A: a) K_2CO_3, Boc_2O, THF, H_2O, room temp. (66%); b) *N*-Boc-2-bromoethylamine, DBU, MeCN, μw 65 °C (57%); c) HCl 4 M in dioxane, room temp. (71%). B: d) *N*-Boc-ethylenediamine, EDC, DCM, room temp., (48%); e) *N*-hydroxyphthalimide, DBU, MeCN, μw 65 °C (87%); f) hydrazine hydrate, DCM, MeCN, μw 65 °C (98%); g) *N*-Boc-*N*-methyl hydroxylamine or *N*-Boc-*N*-benzylhydroxylamine (**1**), DBU, MeCN, μw 65 °C [**Boc(M-AMB)** 45%], [**Boc(B-AMB)** 90%]; h) HCl 4 M in dioxane, room temp. (**AMB** 99%), (**M-AMB** 83%), (**B-AMB** 94%).

dioxane, hence greatly facilitating its isolation as the HCl salt by centrifugation. The synthesis of the linkers **AMB**, **M-AMB** and **B-AMB** commenced with the preparation of the common intermediate **2** by amide bond formation between 4-(chloromethyl)benzoic acid and *N*-Boc-ethylenediamine[26] in the presence of EDC as coupling reagent (Scheme 2, B). The linker **AMB** was prepared following a Gabriel-type synthesis scheme. The benzyl chloride **2** was treated with *N*-hydroxyphthalimide in the presence of DBU with microwave heating giving benzyl phthalic oxy-imide intermediate, then treatment with hydrazine liberated the insoluble phthalhydrazide, thus unmasking the aminooxy moiety of the desired **Boc(AMB)** in high yield. Final Boc removal from the primary amine in hydrochloric dioxane furnished **AMB** as the hydrochloride. Only two steps led from **2** to the remaining linkers **M-AMB** and **B-AMB**. First, the chloride in **2** was substituted by *N*-Boc-*N*-methylhydroxylamine or *N*-Boc-*N*-benzylhydroxylamine (**1**) to obtain the fully Boc-protected intermediates **Boc(M-AMB)** and **Boc(B-AMB)**, respectively. Finally, our standard Boc deprotection scheme in HCl/dioxane allowed the isolation of pure **M-AMB** and **B-AMB** linkers as the chloride salts in high yields.

Model Glycoconjugates: Next, we focused on the preparation of glucose conjugates for all the five linkers presented in Figure 1. These conjugates were chosen to serve as model compounds in order to study their anomeric configuration and their hydrolytic stability. We tested different reaction mixtures, ranging from slightly acidic aqueous buffers to mixtures of polar organic solvents and acetic acid. We could notice that a change in solvent mixture had little or no impact on the yield of conjugate formation. Furthermore, we could clearly observe that, given the same reaction conditions, all the four *N*-substituted linkers consistently gave lower amounts of conjugates compared **AMB** linker. Ultimately, the conjugation reactions were performed in milligram scale in mixtures of methanol and acetic acid at room temperature. Intermediate peracetylation, in pyridine once the conjugation reactions had reached equilibration, served to facilitate the chromatographic separation of the conjugates from the starting materials. Straightforward Zemplén deacetylation allowed us to obtain the target glucose conjugates **Ac(B-AE)Glc**, **Boc(AMB)Glc**, **Ac(M-AMB)-Glc** and **Ac(B-AMB)Glc** in high purity (Figure 3, A). **Boc(AMB)** was used for conjugation instead of **AMB** because peracetylation would also acetylate the linker amino group. As the aliphatic **M-AE** linker structure is devoid of UV-absorbing moieties, we had the need to tag its glucose conjugate with a chromophore in order to later monitor the hydrolytic process by HPLC fitted with online UV/Vis detector. This was achieved by subjecting the crude glucose-linker conjugate to one equivalent of *N*-(benzoyloxy)succinimide[27] (equimolar amounts to linker) in pyridine, thus benzoylating the primary amine. Addition of excess acetic

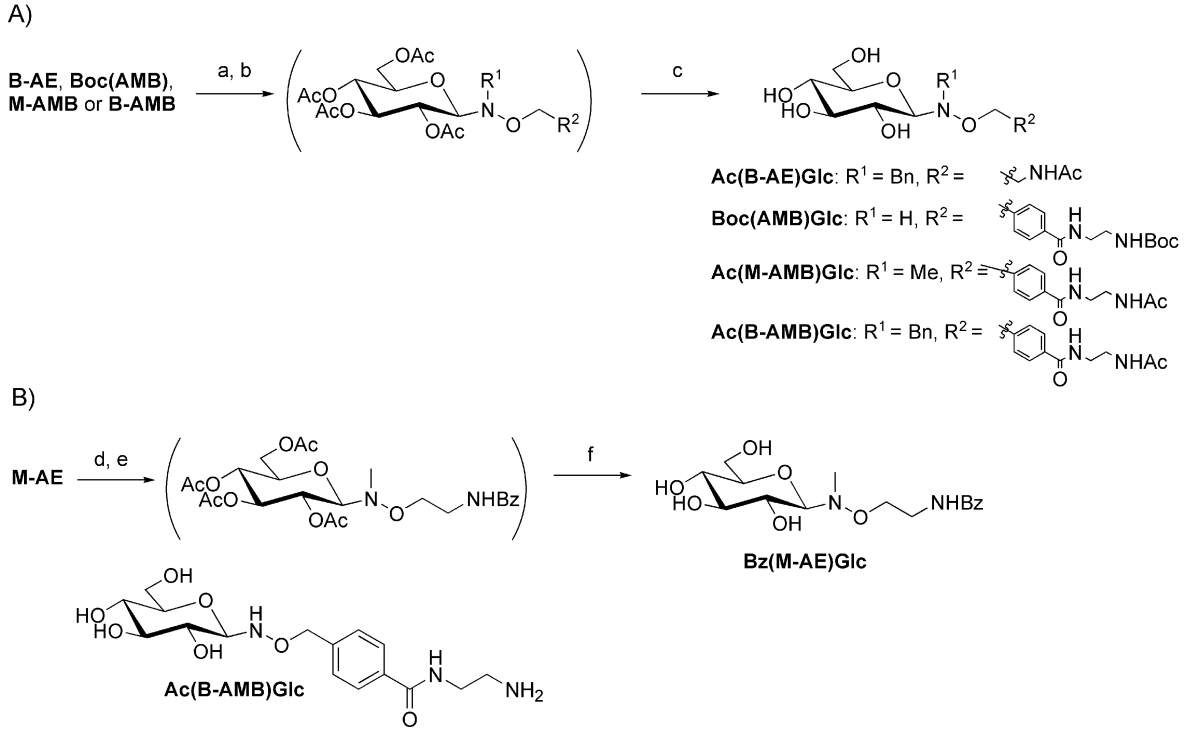

Scheme 3. Preparation of model glucose conjugates for studies of their hydrolytic stability. A: a) Glucose (5 equiv.), MeOH-AcOH (5:1), room temp.; b) Ac_2O (excess), pyridine room temp.; c) MeONa, MeOH, room temp., [**Ac(B-AE)Glc** 59%, 3 steps], [**Boc(AMB)Ac** 74%, 3 steps], [**Ac(M-AMB)Glc** 49%, 3 steps], [**Ac(B-AMB)Glc** 35%, 3 steps]. B: d) Glucose (1.1 equiv.), MeOH/AcOH (5:1), room temp.; e) 2,5-dioxopyrrolidin-1-yl benzoate (1 equiv.), pyridine, room temp., 12 h then Ac_2O (excess); f) MeONa, MeOH, room temp. (**Bz(M-AE) Glc** 22%, 3 steps). Note: for compound **Boc(AMB)Glc** only β-pyranose ring-chain tautomer is shown for simplicity.

anhydride led to peracetylation of the crude mixture en route to isolation of pure **Bz(M-AE)Glc** in 22% overall yield, as described previously for the other linker types (Scheme 3, B). The yield of **Bz(M-AE)Glc** was comparatively low because the coupling reaction at equilibration still contained significant amounts of free linker, which competed for benzoylation with the desired conjugate.

The five glucose conjugates presented in Scheme 3 were characterized in order to determine their configuration and conformation. In accordance with previously reported spectroscopic data,[18b,23,25] for glucose conjugates of *N*-methylhydroxylamines, we found that the conjugates **Bz(M-AE)Glc** and **Ac(M-AMB)Glc** were obtained in the $^4C_1$ conformation with complete diastereoselectivity as β-pyranose forms. Also compound **Boc(AMB)Glc**, was in agreement with our prediction[28] as NMR spectroscopic analysis revealed the presence of both open-chain and ring-closed tautomers as follows: (*E*)-oxime/(*Z*)-oxime/β-pyranose ring-chain in 60:20:20 ratio respectively. No structural characterization has been previously reported in the literature concerning conjugates between carbohydrates and *N*-benzylhydroxylamines. HPLC-MS analysis of both crude **Ac(B-AE)Glc** and **Ac(B-AMB)Glc** showed a single product peak, which bode well for the formation of single tautomer with complete diastereoselectivity. Further analysis by 1D and 2D NMR spectroscopy corroborated the presence of the conjugates with $^4C_1$ conformation exclusively as β-pyranose forms (see Supporting Information).

Hydrolytic Stability of Glucose-Linker Conjugates

In recent years the chemoselective coupling between the reducing end of glycans and *N*-alkyl hydroxylamines has been exploited for different types of applications that extend beyond glycochip fabrication.[29] Nevertheless, data concerning the stability towards hydrolysis of *N*-substituted aminooxy-based glycoconjugates is scantily present in the literature.[30] During the preparation of this paper, Nitz and co-workers published a survey addressing the hydrolytic stability of glycoconjugates of xylose, glucose and *N*-acetylglucosamine with two different types of *N*-methylhydroxylamine derivatives which showed that conjugates formed from relatively electron-rich monosaccharides hydrolyzed more rapidly.[31] Our goal was to perform a thorough mapping of the hydrolytic stability of linker-glucose conjugates shown in Scheme 3 in solutions ranging from pH 3–5 at one pH unit intervals. The glycoconjugate concentration throughout the experiment was set at 1 mM and the solutions were incubated at room temperature. The hydrolytic events were monitored at intervals by HPLC with UV/Vis detection over 4 d. UV absorption of the linkers was the same as their corresponding conjugates (see Supporting Information). We monitored the peak areas [at 230 nm for all but **Ac(B-AE)Glc** for which 215 nm was used instead] to estimate the ratio between conjugate and linker as percent of conjugate remaining according to the formula [$A_{conjugate}/(A_{conjugate} + A_{linker})$] for each of the three buffer systems. The hydrolysis of all the conjugates fitted well to a pseudo first-order process (see Supporting Information) that allowed the calculation of the conjugate's half-lives as reported in Table 1 (at pH 7 all conjugates showed no detectable hydrolysis throughout the course of the study).

Table 1. Stability (half-lifes) towards hydrolysis of glycan-linker conjugates (study performed at room temperature).

	pH 3 $t_{(1/2)}$ [h]	pH 4 $t_{(1/2)}$ [h]	pH 5 $t_{(1/2)}$ [h]
Bz(M-AE)Glc	5.4	28	215
Ac(B-AE)Glc	23	114	755
Boc(A-MB)Glc	24	86	605
Ac(M-AMB)Glc	6.5	34	250
Ac(B-AMB)Glc	35	168	765

As expected, the rates of hydrolysis for all the conjugates were pH-dependent, thus for a given specie, the lower the pH the faster the hydrolysis. The hydrolysis of conjugates formed with secondary *N*-methylhydroxylamines **Bz(M-AE)Glc** and **Ac(M-AMB)Glc** occurred four- to fivefold faster than the oxime **Ac(AMB)Glc**, in the pH range investigated. By contrast, the stabilities of the *N*-benzyl hydroxylamine-based conjugates were much higher, even slightly higher than **Ac(AMB)Glc**. Furthermore, given the same substituent at nitrogen, there was marginal, yet noticeable increased stability in favor of the *O*-benzyl vs. the *O*-alkyl conjugates throughout the pH range investigated [**Bz(M-AE)Glc** vs. **Ac(M-AMB)Glc** and **Ac(B-AE)Glc** vs. **Ac(B-AMB)Glc**]. One possible explanation could be that it is due to the different electronic effects that the different substituents exert upon the linker aminooxy moiety, both on nitrogen and oxygen. Substituents on nitrogen though, have a more pronounced impact on the conjugate stability as opposed to the ones on oxygen. In view of this, the remarkable stability of glucose conjugates of *N*-benzyl linkers could be ascribed to the slightly negative inductive effect of the benzyl moiety, as opposed to the methyl moiety, which, on the other hand imparts a slightly positive inductive effect. In accordance to what was reported recently by Nitz and co-workers,[31] we assume that upon exposure of the conjugates to acid environment, an equilibrium between neutral and nitrogen protonated forms is established. Protonation opens the conjugate yielding an oxyiminium cation, in which C_1 is joined to the positively charged nitrogen via a double bond. The oxyiminium ion is the intermediate susceptible of nucleophilic attack from a water molecule in the rate-determining step of the hydrolytic process. *N*-benzyl conjugates are more electron deficient, thus less prone to protonation compared to their *N*-methyl analogues, which in turn makes them more resilient towards hydrolysis.

Preparation of Glycan-Liker Conjugates for Microarray Fabrication

The results obtained for the chemoselective couplings of the five linkers with glucose bode well for their applicability to other reducing glycans. We aimed to devise a methodol-

ogy that could allow straightforward purification of the glycoconjugates. To this end, we decided to focus on the three linkers of the *O*-benzylic series, **AMB**, **M-AMB** and **B-AMB** as they proficiently absorb UV light, which allowed tracing during chromatography and the linkers' aromatic moiety could aid retention of the conjugates in reverse-phase columns, which are normally not well suited for highly hydrophilic compounds such as glycans. Moreover, as the linkers share the same core structure, it would be possible to rationalize their different performances (in terms of glycoconjugate formation, purification and on-chip behavior towards GBPs probing) to the substitution pattern at the nitrogen of the aminooxy moiety.

We then selected lactose, *N*-acetyllactosamine and 1,2-α-mannobiose to produce a small ensemble of conjugates with each of the selected linkers. We focused on disaccharides, as the binding event with GBPs would occur in direct proximity of the attachment point between glycan and linker (i.e. the reducing end), thus we would be able to determine the role of steric effects as well as possible anomeric heterogeneity. Higher order oligosaccharide could potentially level off any differences as the binding events typically occur further away from the anchoring point. Furthermore, *N*-acetyllactosamine presents *N*-acetylglucosamine as reducing-end hexose, thus serving as a model substrate for *N*-linked glycoproteins and glucoaminoglycans. Mannobiose, on the other hand, could serve as model compound for, e.g. membrane glycoproteins, which have a "core oligosaccharide" structure which includes α-linked mannose residues. Finally, lactose bears glucose as reducing unit, which was our model glycan for the hydrolysis studies outlined above but also serve as a model for glycolipids (Glc-Cer).

The chemoselective coupling reactions between linkers and glycans were carried out in aqueous ammonium acetate buffer at pH 4.5, in order to maximize the reaction rate.[32] The equilibrium constants for such kind of condensations are moderate,[31,32] and high yields are often obtained by performing the reactions under concentrated conditions. However, this cannot be used for complex glycans derived from natural sources, as they are difficult and expensive to isolate in large amounts. To this end, we preferred to operate with excess of linker and to minimize the reaction volumes. In our standard protocol, the reaction volumes were kept between 100 and 200 μL, the glycan concentration was set at 20 mM whilst the linkers were present in either threefold (**M-AMB** and **B-AMB**) or 1.5-fold (**AMB**) excess and gentle heating was applied (37 °C). Thus, only a few micromol of glycans were actually used per reaction.

Monitoring of the coupling reactions by HPLC highlighted differences in reactivity among the three linkers, which were analyzed qualitatively. First, reactions involving the unsubstituted aminooxy linker **AMB** reached thermodynamic equilibrium faster (within 24 h vs. 48–72 h) and consistently provided higher conversions of conjugate product (given the same glycan) compared to the *N*-substituted variants **M-AMB** and **B-AMB**. Second, in line with the result obtained with the glucose conjugates, the **B-AMB** linker gave lower conversions of conjugate compared to **M-AMB** with all the glycans prepared. This lower reactivity could be due to a combination of steric crowding and negative inductive effect exerted onto the aminooxy moiety by the benzyl group. Third, disaccharides showed the following order of reactivity with the *N*-substituted linkers **M-AMB** and **B-AMB**: lactose > *N*-acetyllactosamine >> 1,2-α-mannobiose. These observations are in accordance with the results reported by Peri et al.[23] for the formation of *N*-methylhydroxylamine conjugates. Interestingly, the *N*-unsubstituted **AMB** linker, gave approximately the same product conversions with 1,2-α-mannobiose and lactose, while the *N*-acetyllactosamine was the least reactive.

The use of buffered eluents (10 mM NH_4OAc, pH 5.8) with mixed-mode HILIC column operated in RP (capable of polar and hydrogen bonding interactions) proved to be particularly well suited both for the monitoring of the coupling reactions as well as purification of glycoconjugates. In the instances when conjugation reactions were not proceeding with high isomeric selectivity, it became often possible to neatly observe well resolved multiple product peaks on the chromatogram. No attempts were made to isolate separately different isomers (ring-chain tautomers) of the target conjugates, if present. Furthermore, as only few micromol of material were required from each analyte for the preparation of several microarray slides, we achieved proficient purification of sufficient amount of conjugates by using the same analytical HPLC columns employed for reaction monitoring (Figure 2).

The fractions containing the target conjugates were then pooled, freeze-dried and taken up with print buffer in order to furnish the stock solutions to be arrayed on chip. The concentration of the different stock solutions was conveniently estimated via calibration curves built from pure linker. The purification of the reaction mixtures containing **AMB** was particularly challenging due to the poor resolution between product and free linker peaks. We could conveniently circumvent the problem by capping the excess of linker as the acetone oxime.[33] The addition of acetone (10 equiv.) to crude reaction mixture at equilibration resulted in the appearance of a new peak at longer retention times within 1 h (identified as **AMB-acetone** oxime by ESI-MS), without having any detectable deleterious effect upon the target glycan conjugates (Figure 2, C).

The ease of use of our linkers for glycan microarray fabrication would improve further if pure glycan-linker conjugates were obtained without the need of HPLC chromatography. We reasoned that purification by extraction of the excess of linkers with water-immiscible organic solvents could be a viable option as the linkers might display a sufficient degree of lipophilicity to allow partition into the organic phase. In such case, the crude reaction mixture would eventually contain only the desired conjugate and some unreacted glycan molecules. The latter can be considered irrelevant as most glycans neither affect concentration estimate of the target conjugate (i.e. residual free glycan is devoid of UV absorption) nor react with NHS-coated slides, because no primary amines are present. To test our hypothesis, the reaction mixtures at equilibration were freeze-dried and the

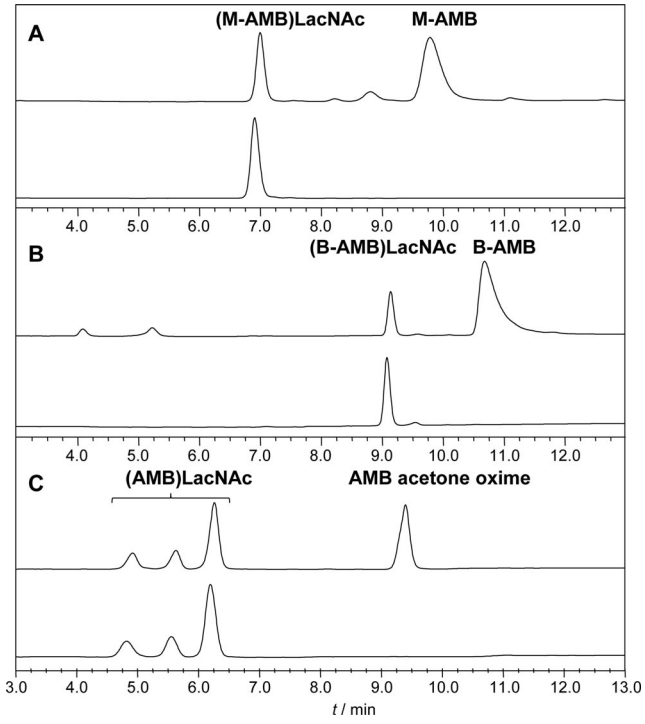

Figure 2. RP-HPLC chromatograms (230 nm) with a mixed-mode Acclaim HILIC (Dionex) column of the conjugation reaction between *N*-acetyllactosamine (LacNAc) and (A) **M-AMB**, (B) **B-AMB** and (C) **AMB** at equilibration (top trace in each panel) and after HPLC purification (bottom trace in each panel). In panel C, three product peaks are visible corresponding to different isomers of (**AMB)LacNAc**, as corroborated by online ESI-MS analysis.

residue taken up in 100 mM NH_4OAc buffer, pH 9 so that the linkers primary amino group could be rendered predominantly in the neutral form. Then, the organic solvent was applied in iterated rounds of extractions. HPLC analysis of both water and organic phase showed that it was indeed possible to remove excess of **B-AMB** linker from all the three reactions containing the different disaccharides and, most importantly, no trace of target conjugates was detected in the organic phase. Dichloromethane (DCM) was found to be more suited for extraction, also by virtue of its limited wettability. Thus, the amount of free **B-AMB** left in the water phase was down to impurity level. On the other hand, excess of **M-AMB** and **AMB** linkers were only marginally removed from the respective reaction mixtures even when the extractions were iterated several times (>10) and for many minutes (>60) each time.

In order to evaluate the extraction procedure, a condensation reaction containing 1 mM of *N*-acetyllactosamine and 50 mM of **B-AMB** was set up. Upon equilibration and switch to the basic buffer, repeated extractions were undertaken. To our delight, even with such a high excess of **B-AMB** present, the extraction procedure proved to be successful. As shown in Figure 3, after five extraction rounds, the amount of free **B-AMB** was greatly reduced and after eight extractions it was just above detection levels. Moreover, control analysis of the organic phases showed no traces of the target conjugate.

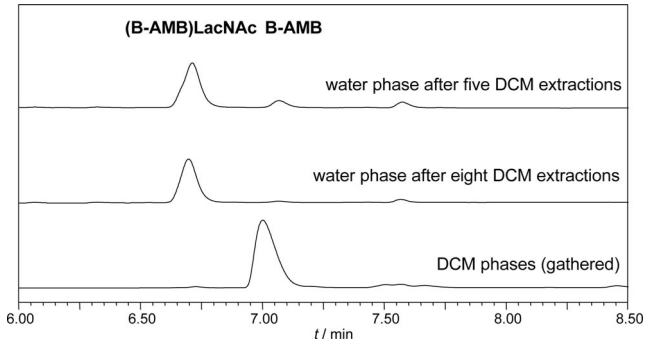

Figure 3. RP-HPLC separations with Jupiter C4 (Phenomenex) column (recorded at 254 nm) of the water phase after five (top) and eight (middle) DCM extractions. Only **B-AMB** linker was detected in the DCM phase (bottom). Peak assignment corroborated by online ESI-MS.

On-Chip Glycan-Linker Conjugates Assay with Lectins

With our ensemble of disaccharide-linker conjugates in hand, we probed their ability to interact with biologically relevant lectins in a microarray. The conjugates were spotted with a robotic microarrayer on Nexterion Slides H at four different concentrations, with a fivefold dilution gap from one another, namely 250, 50, 10 and 2 μM. Each slide housed 16 identical arrays, which displayed the sugar probes in four replicate per dilution.

The on-chip behavior of the printed conjugates was assessed by means of four biotin-labeled lectins, Con A, RCA I, ECA and WGA, all applied at 10 μg/mL. Visualization of bound lectins was then achieved by treatment with Streptavidin-Alexa488 conjugate; in Figure 4 the histograms representing the average relative fluorescence units (RFU) recorded from microarray scanning are shown. Rewardingly, all the lectins tested were able to successfully bind only to their cognate ligands, while otherwise only fluorescence signals down to background levels were recorded. This ruled out the occurrence of non-specific binding events between lectins and linker moieties on microarray. **M-AMB** and **B-AMB** conjugates displayed very similar performances with the α-mannose binding lectin Con A,[34] the β-galactose binding lectin RCA I[35] and the LacNAc-binding lectin ECA.[36] Moreover, all the batches of **B-AMB** conjugates purified by extraction proved to be properly spotted and recognized by lectins, hence furnishing fluorescence readouts which were in line with their HPLC-purified counterparts.

Interestingly, when the glycochips were assayed with WGA,[37] in order to elicit binding with *N*-acetylglucosamine, which was internally presented in *N*-acetyllactosamine conjugates, only **(M-AMB)LacNAc** was successfully recognized while **(B-AMB)LacNAc** was not detected. The chitopentaose conjugate of **AMB**, **(AMB)(GlcNAc)$_5$**, was prepared in the same fashion described above for the other conjugates, and was spotted as a positive control; as expected clear binding with WGA was recorded. Then, the isomeric nature of the linkage between **B-AMB** and *N*-acetyllactosamine was investigated by preparing milligram

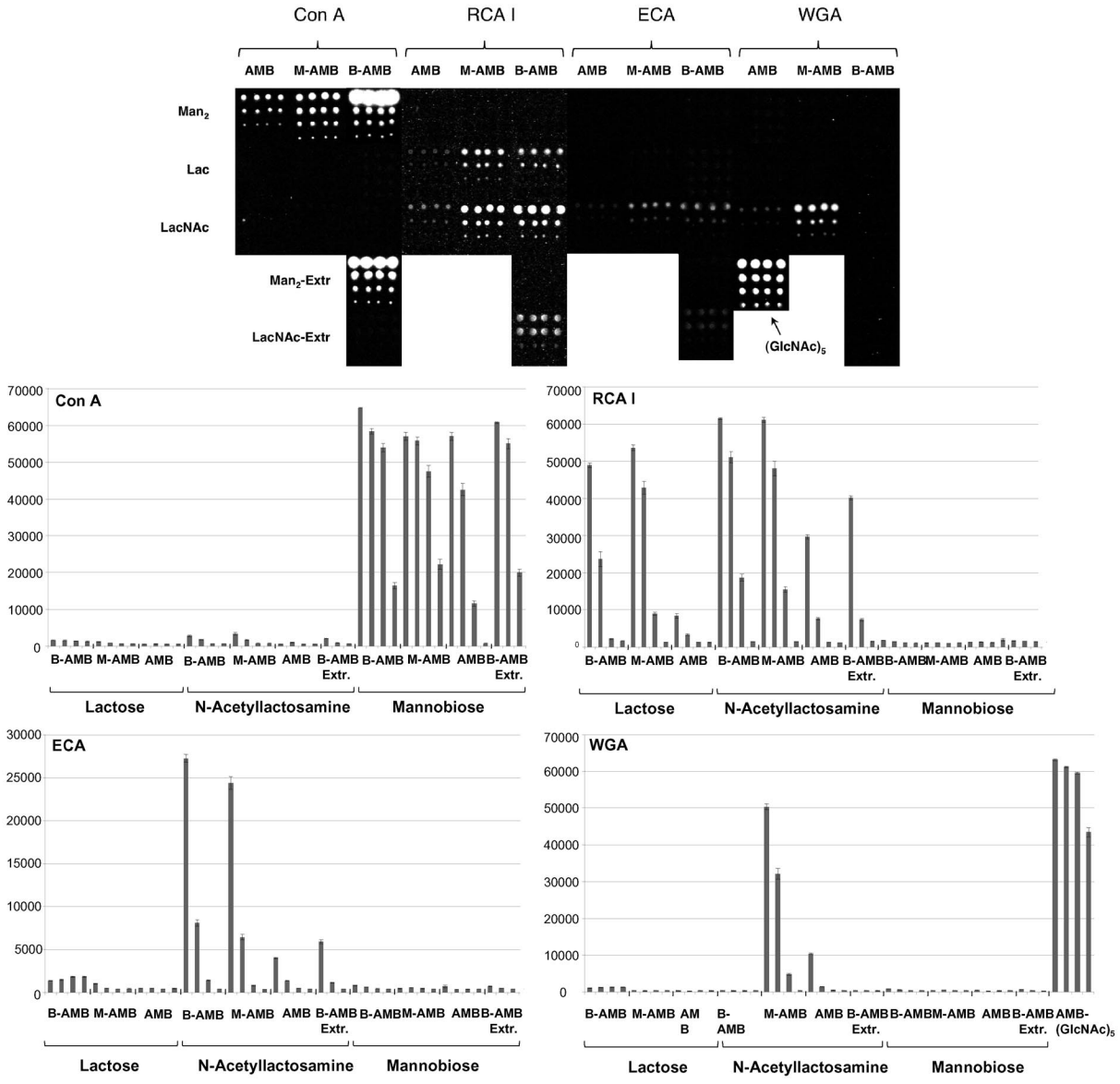

Figure 4. Microarray image after fluorescent scanning (top) and histograms representing average relative fluorescence units (RFU) recorded from microarray scanning (bottom). The fluorescence values (the mean fluorescence value arising from each spot was used) are the average of 16 spot replica per conjugate on a single slide and no background subtraction was performed. The spot size was determined by ScanArray Express analysis program with the adaptive circle method (nominal diameter set at 130 μm, minimum and maximum spot diameter 60% and 160% of nominal, respectively). All conjugates printed at 250, 50, 10 and 2 μM (left to right), except **(B-AMB)LacNAc Extr.** printed in at 50, 10 and 2 μM (50 μM printed on two rows in image) and **(B-AMB)Man2 Extr.** printed in at 100, 50, 10 and 2 μM (in histograms 100 μM not shown).

amounts of pure **Ac(B-AMB)GlcNAc** conjugate (see Supporting Information). NMR spectroscopic characterization revealed that the conjugate was in pyranose form with β-conformation, the same as reported for GlcNAc conjugates with *N*-methylhydroxylyamine-type linkers such as **M-AMB**.[23] Accordingly, we speculate that the lack of binding between **(B-AMB)LacNAc** and WGA is related to the presence of *N*-benzyl substituent in direct proximity with the target glycan ligand. Such bulky and hydrophobic moiety might somehow prevent the ligand to achieve efficient docking into the binding pocket of this specific lectin.

It is remarkable that all the different **AMB** conjugates exhibit lower fluorescent signals, i.e. lower binding, upon probing with lectins compared to respective **M-AMB** and **B-AMB** conjugates throughout the dilution range. These differences are less apparent with Con A, but become quite clear with the remaining three lectins. As an example, if we consider the signal arising from the spots at 250 μM, a concentration at which it is reasonable to assume reaction of all the reactive-NHS ester sites on Nexterion Slide H by the glycan conjugates,[38] **AMB** conjugates approximately provide only 20% of the signal in three instances [i.e.

(AMB)Lac with RCA I, **(AMB)LacNAc** with ECA and WGA] compared to the corresponding **M-AMB** and **B-AMB** conjugates. We believe that the observed limited interaction of **AMB** conjugates with lectins, as opposed to **M-AMB** and **B-AMB** conjugates, are due to the fact that the glycans are presented by the former linker with anomeric heterogeneity (oxime tautomer), where the open-chain isomer is the one most represented (approximately 75% for both lactose and *N*-acetyllactosamine[39] and close to 100% with mannose[40]) whereas the latter give rise only to ring-closed conjugates.[41] Such rationalization is in line with findings of Shin et al.[42] who, after solution NMR spectroscopic and on-slide reactivity studies, related higher fluorescence signals upon lectin binding for glycans applied to hydrazide vs. hydroxylamine coated glass slides to the nature of the anomeric linkage established on the surface. The preferential formation of ring-closed conjugates with the hydrazide linking moieties resulted in higher signals. Furthermore, Cummings and co-workers recently reported that when lactose was conjugated to a bifunctional linker via reductive amination (thus forming exclusively open-chain structure at the glucose unit) and subsequently spotted onto Nexterion Slide H, no binding was observed when probing with RCA I.[43]

As a final experiment, it was investigated how the surface-bound glycoconjugates responded to hydrolytic conditions. After the glycochip was printed (same setup as above) and blocked, identical subarrays were subjected to either phosphate buffer 100 mM, pH 3 or to print buffer, pH 8.6, and incubated. After 6 h, pH 3 buffer was removed from some subarrays, which were backfilled with print buffer. After 24 h of incubation, all the wells were emptied and the slide washed and treated with RCA I. Subsequent treatment with Streptavin-Alexa488 conjugate and fluorescent scanning allowed us to assess the response of the glycoconjugate to hydrolytic conditions. RCA I was chosen for probing to obtain information from the lactose glycoconjugates with **M-AMB** and **B-AMB**, which present glucose at the reducing end, to see how these related to the hydrolysis study in solution. Thus the lactose conjugates could be compared with *N*-acetyllactosamine conjugates (with *N*-acetylglucosamine at the reducing end), as solution studies[31] had found *N*-methylhydroxylamine conjugates with *N*-acetylglucosamine to be more stable than with glucose. In Figure 5 the results from microarray scanning of the 250 μM print are presented as bar graph; for each conjugate the data presented was normalized to its respective fluorescent readout collected after lectin probing from the subarrays incubated in print buffer for 24 h, conditions at which we assume the hydrolysis to be negligible. The results are in agreement with the solution studies, since the overall higher stability of **B-AMB** vs. **M-AMB** conjugates was observed on-chip as well. If we consider the lactose series, **(M-AMB)Lac** appears to be hydrolyzed nearly to completion already after 6 h, whereas RCA I binding to **(B-AMB)Lac** is unchanged on the 6 h subarray and reduced down to 20% on the 24 h subarray. Furthermore, given the same linker, *N*-acetyllactosamine conjugates provided higher normalized signals compared to the lactose ones (see **M-AMB** and **B-AMB** conjugates at 24 h in Figure 5), indication of more pronounced stability of the **LacNAc** conjugates to hydrolysis. Comparing linkers, **(B-AMB)LacNAc** conjugates displayed superior stability compared to **(M-AMB)LacNAc**, as it can easily be visualized in Figure 5 from the probing of the 24 h incubation subarrays: **(M-AMB)LacNAc** signal is greatly diminished while **(B-AMB)LacNAc** furnished readouts in line with the subarrays incubated in print buffer. As this is only an indirect measure of the degree of hydrolysis on-chip, comparable levels of fluorescence output between a given conjugate in a subarray incubated at pH 3 and one incubated at pH 8.6 did not necessarily mean that all the conjugates were left unchanged from acid treatment, but rather that on-slide the conjugate density was still sufficient to guarantee that the coupled assay applied for probing (i.e. RCA I/Strptavin-Alexa488) furnished very similar fluorimetric readout.

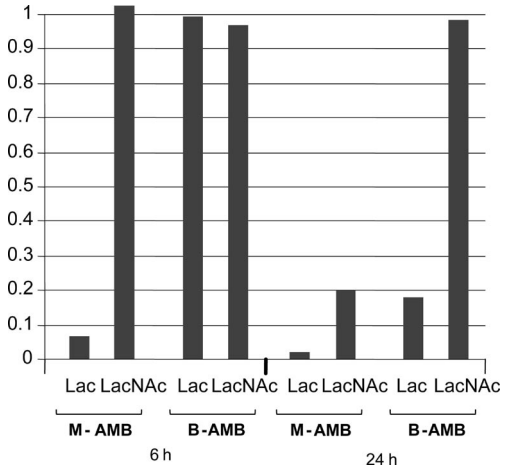

Figure 5. Histogram of the on-chip hydrolysis study at pH 3. The values for each conjugate type (250 uM spots) were normalized to their respective mean fluorescent readouts collected upon incubation with print buffer for 24 h. Values are the mean of two set of identical experiments, standard deviation between 4% and 7%.

Conclusions

We have studied five bifunctional aminooxy-type linkers, four of which were new, for the chemoselective capture of unprotected oligosaccharides in solution followed by construction of covalent microarrays. The linkers displayed a diversified *N*- and *O*-substitution pattern at the aminooxy moiety, where different combinations of *O*- and *N*-alkyl and benzyl substituents were in place. Conjugates with glucose as a model system were characterized by NMR spectroscopy, and their hydrolytic stability in solution (pH 3–5) was assessed. Conjugates with *N*-benzyl-substituted aminooxy-type linkers, **B-AE** and **B-AMB**, were characterized for the first time and proved to yield glucose conjugates in closed-ring β-pyranose form with high diastereoselectivity. The hydrolytic events fitted well with pseudo-first order kinetics, thus the half-lives of the conjugates were calculated.

N-methyl-substituted conjugates, **Bz(M-AE)Glc** and **Ac(M-AMB)Glc**, were the least stable, whereas *N*-benzyl-substituted conjugates, **Ac(B-AE)Glc** and **Ac(B-AMB)Glc**, displayed stabilities similar or superior to that of the oxime-type conjugate **Boc(AMB)Glc** throughout the pH range studied. The structurally related and UV-active linkers **AMB**, **M-AMB**, and **B-AMB** were selected, and each one was conjugated with lactose, *N*-acetyllactosamine, and 1,2-α-mannobiose for microarray fabrication. Convenient purification was achieved with RP HPLC (mixed-mode HILIC column) and by DCM extraction (**B-AMB** linker only). Finally, microarrays fabricated on NHS-activated slides were probed with four lectins, Con A, RCA I, ECA, and WGA. All conjugates were able to give efficient binding exclusively to their cognate lectin. Remarkably, conjugates of the *N*-substituted linkers **M-AMB** and **B-AMB** gave similar fluorescent readouts throughout the whole range of concentrations spotted with Con A, RCA I, and ECA, but not the *N*-acetylglucosamine binding lectin WGA, which bound proficiently to (**M-AMB**)**LacNAc** yet not to (**B-AMB**)-**LacNAc**. We hypothesize this to be due to the deleterious presence of the benzyl substituent in direct proximity to the WGA binding epitope. **AMB** conjugates upon lectin binding provided fluorescent signals consistently inferior compared to those of the **M-AMB** and **B-AMB** linkers for all the four lectins probed and throughout the spotted concentration range. Given that the linkers share the same structural framework, the immobilization efficiency on slide are likely to be the same, and therefore we conclude that the weaker readouts from **AMB** conjugates are due to their structural heterogeneity at the anomeric center. The open chain form was the predominant isomer with all the glycans tested, whereas both **M-AMB** and **B-AMB** furnished closed-ring conjugates. Our work highlights that, when addressing glycoconjugates with short oligosaccharides, it is crucial to produce structures that mimic their parent natural compounds. Loss of structural integrity, in form of open-chain oxime conjugates or the presence of bulky substituents at the anomeric center (such as the benzyl moiety), can in this system hamper the occurrence of the desired binding event.

Experimental Section

Materials and Analysis: All chemicals were purchased from Sigma–Aldrich Denmark. Biotin labelled lectins purchased from Vector Labs (Peterborough, UK) and Streptavis-Alexa488 conjugate purchased from Invitrogen Denmark. MilliQ water was used for all aqueous preparations. All solvent ratios are v/v. ^{1}H, ^{13}C, APT, HSQC, and COSY NMR spectra were recorded on a Bruker Avance 300 spectrometer with a BBO probe. The chemical shifts are referenced to the residual solvent signal. Assignments were aided by COSY, HSQC, and APT experiments. Mass determination (high resolution MS, HR-MS) was performed on a Micromass LCT instrument with an ESI probe. Analytical HPLC was performed on a Dionex Ultimate 3000 system with Chromeleon 6.80SP3 software. Unless otherwise stated, two sets of reverse-phase (RP) elution conditions were used. **Elution Condition 1:** 1.0 mL/min linear gradient flow of B (MeCN, 0.1% formic acid) in A (H_2O, 0.1% formic acid) 12 min; analytical columns used were either Phenomenex Gemini™ C-18, 50 × 4.60 mm, 3 μM, 110 Å or Phenomenex Jupiter™ C-4, 150 × 4.60 mm, 5 μM, 300 Å. **Elution Condition 2:** 1.0 mL/min linear gradient flow of D (9:1, v/v, MeCN/NH_4OAc 100 mM, pH 5.8) in C (NH_4OAc 10 mM, pH 5.8) over 15 min; analytical columns used were either Phenomenex Hydro™ 150 × 3.0 mm, 4 μM, 80 Å or Dionex Acclaim™ Mixed-Mode HILIC-1 150 × 5 mm, 5 μM, 120 Å. Unless otherwise stated, yields refer to chromatographically isolated and spectroscopically pure materials. Commercially available starting materials were used as received without further purification. Dry-column chromatography was performed using Merck silica gel 60 (230–400 mesh). Microarray printing was performed by robotic contact printing with a BioRobotics Microgrid II (Genomics Solutions) fitted with Stealth 3B Micro Spotting pins (Telechem International ArrayIt Division). Source plates were prepared with BD Falcon Microtest™ 384-well 30 μL assay plates (BD Biosciences, Le Pont De Claix, France). Microarrays were visualized in a ProScanArray HT Microarray Scanner (Perkin–Elmer) and image analysis performed with ProScanArray Experess 4.0 (Perkin–Elmer).

***N*-Boc-*N*-Benzylhydroxylamine (1):** *N*-Benzylhydroxylamine hydrochloride (1000 mg, 6.26 mol) was placed in a round-bottom flask and dissolved in a 1:1 mixture of THF and water (10 mL). After cooling on ice bath, potassium carbonate (432 mg, 3.13 mol) was slowly added to the solution and gas evolution was observed. Once gas evolution ceased, a solution of di-*tert*-butyl dicarbonate (1500 mg, 6.9 mol) in THF (15 mL) was added dropwise to the mixture and stirring was continued for 2 h at 0 °C and then at room temperature overnight. Then the solution was concentrated in vacuo and the residue taken up in DCM (50 mL) and washed with water (3 × 800 mL) and brine (1 × 80 mL). The organic solution was dried with $MgSO_4$, the solvent removed in vacuo and the resulting residue absorbed onto celite. Purification with vacuum-column chromatography (EtOAc 0 to 50% in heptane) gave the pure product **6** in 66% yield as colorless crystalline solid. ^{1}H NMR (300 MHz, $CDCl_3$): δ = 7.35–7.33 (m, 5 H, ArH), 5.98 (s, 1 H, *NH*), 4.65 (s, 2 H, CH_2Ar), 1.50 [s, 9 H, $(CH_3)_3$-C] ppm. ^{13}C NMR (75 MHz, $CDCl_3$): δ = 156.6, 136.3, 128.5, 128.1, 127.6, 82.3, 53.9, 28.3 ppm.

2-(*N*-Boc-*N*-Benzylaminooxy)-*N*-Boc-ethanamine [Boc(B-AE)]: An oven-dry microwave vial provided with magnetic flea was loaded with *N*-Boc-*N*-benzylhydroxylamine (400 mg, 1.78 mmol, 1.0 equiv.) and *tert*-butyl 2-bromoethylcarbamate (460 mg, 2.0 mmol, 1.15 equiv.) under Ar. Acetonitrile (5 mL) was added, rapidly giving a clear solution. Finally DBU (330 μL, 2.23 mmol, 1.3 equiv.) was added dropwise via syringe, the vial was sealed and microwave irradiation was undertaken for 40 min at 65 °C. The volatiles were then removed in vacuo and the resulting residue taken up in 30 mL of DCM and extracted 2 × 30 mL of HCl 0.5 M, 2 × 30 mL of NaOH 1 M and 1 × 30 mL of saturated $NaHCO_3$ aqueous solution. The organic layer was concentrated to dryness and the residue absorbed on celite. Purification with vacuum-column chromatography (EtOAc 0 to 50% in heptane) gave the pure product **7** (371 mg, 57%) as a colorless oil. ^{1}H NMR (300 MHz, $CDCl_3$): δ = 7.34–7.31 (m, 5 H, ArH), 5.28 (br. s, 1 H, NH) 4.58 (s, 2 H, CH_2Ar), 3.75 (t, J = 4.8 Hz, 2 H, CH_2ON), 3.24 (dd, J = 4.8, 10 Hz, 2 H, CH_2NH), 1.49 [s, 9 H, $(CH_3)_3$-C], 1.42 [s, 9 H, $(CH_3)_3$-C-] ppm. ^{13}C NMR (75 MHz, $CDCl_3$): δ = 156.8, 155.9, 136.6, 128.4, 127.6, 82.1, 79.1, 77.2, 74.1, 53.6, 38.9, 28.3, 28.2 ppm. HR-MS (ESI): calcd. for $C_{19}H_{30}N_2O_5$ $[M + Na]^+$, 389.2047; found 389.2052.

***N*-(2-Boc-Aminoethyl)-4-(chloromethyl)benzamide (2):** 4-Chloro toluic acid (510 mg, 3.0 mmol) and EDC hydrochloride (632 mg, 3.3 mmol) were placed in a round-bottomed flask and covered in DCM (5 mL). The flask was closed with a septum and *tert*-butyl 2-aminoethylcarbamate (530 mg, 3.3 mmol), dissolved in DCM (2 mL), was added dropwise via syringe. Few seconds after completion of the addition, the reaction mixture became homogeneous whereupon the vial was sealed and placed in the microwave reactor cavity and irradiated at 60 °C for 10 min. Once cooled to room temp. the reaction mixture was diluted with DCM (20 mL) and extracted with 5% citric acid solution (2 × 30 mL), NaOH 1 M (1 × 20 mL) and $NaHCO_3$ (1 × 20 mL) then dried with $MgSO_4$, reduced to dryness in vacuo and the resulting residue absorbed onto celite. Purification with vacuum-column chromatography (EtOAc 0 to 100% in heptane) gave the pure product **2** (448 mg, 48%) as a white solid. ^{1}H NMR (300 MHz, $CDCl_3$): δ = 7.81 (d, J = 8.2 Hz, 2 H, ArH), 7.45 (d, J = 8.2 Hz, 2 H, ArH), 7.23 (br. s, 1 H, *NH*CO), 4.94 [br. s, 1 H, *NH*CO(O)], 4.61 (s, 2 H, CH_2Ar), 3.58 (dd, J = 5, 10 Hz, 2 H, *CH*$_2$NHCO), 3.54 [dd, J = 5, 10 Hz, 2 H, *CH*$_2$NHCO(O)], 1.43 [s, 9 H, (*CH*$_3$)$_3$-C] ppm. ^{13}C NMR (75 MHz, $CDCl_3$): δ = 167.0, 141.0, 134.1, 129.1, 128.6, 127.4, 45.4, 42.3, 39.9, 28.3 ppm. MS (ESI): calcd. for $C_{15}H_{21}ClN_2O_3$ [M + H]$^+$, 312.1; found 312.1.

***N*-(2-Boc-Aminoethyl)-4-[(1,3-dioxoisoindolin-2-yloxy)methyl]benzamide:** An oven-dry microwave vial provided with a magnetic flea was loaded with *N*-hydroxyphthalimide (232 mg, 1.43 mmol) and 3 mL of acetonitrile. Upon dropwise addition of DBU (200 μL, 1.43 mmol) the mixture became a red homogeneous solution. A solution of *tert*-butyl 2-[4-(bromomethyl)phenylamido]ethylcarbamate (300 mg, 0.84 mmol) in 4 mL of acetonitrile was added, the vial was sealed and microwave-heated for 30 min at 65 °C. After irradiation a white precipitate appeared in the reaction mixture. The precipitate was filtered by suction and washed with HCl 0.5 M (2 × 30 mL), NaOH 1 M (2 × 30 mL) and water (2 × 30 mL) and finally dried in the oven at 145C for 1 h thus giving the title compound in 87% yield. ^{1}H NMR (300 MHz, [D$_6$]DMSO): δ = 8.49 (br. t, J = 5.2 Hz, 1 H, NHCO), 7.85 (m, 6 H), 7.59 (d, J = 8.2 Hz, 2 H, ArH), 6.91 [br. t, J = 5.6 Hz, 1 H, *NH*CO(O)], 5.22 (s, 2 H, CH_2Ar), 3.28 (dd, J = 6, 12 Hz, 2 H, *CH*$_2$NHCO), 3.11 [dd, J = 6, 12 Hz, 2 H, *CH*$_2$NHCO(O)], 1.36 [s, 9 H, $(CH_3)_3$-C-] ppm. ^{13}C NMR (75 MHz, [D$_6$]DMSO): δ = 165.8, 162.9, 155.6, 137.0, 134.8, 134.7, 129.1, 128.3, 127.2, 123.1, 78.4, 77.5, 28.1 ppm. HR-MS (ESI): calcd. for $C_{23}H_{25}N_3O_6$ [M + Na]$^+$, 462.16; found 462.25.

***N*-(2-Boc-Aminoethyl)-4-[(*N*-Boc-*N*-methylaminooxy)methyl]benzamide [Boc(M-AMB)]:** *tert*-Butyl 2-[4-(bromomethyl)phenylamido]-ethylcarbamate (171 mg, 0.48 mmol) and *tert*-butyl hydroxy(methyl)-carbamate (82 mg, 0.55 mmol) were treated as described for compound **Boc(B-AE)**. The crude product was absorbed on Celite and purified with vacuum-column chromatography (EtOAc 0 to 100% in heptane) gave the pure product **Boc(M-AMB)** as colorless amorphous solid (90 mg, 45%). ^{1}H NMR (300 MHz, $CDCl_3$): δ = 7.81 (d, J = 8.2 Hz, 2 H, ArH), 7.45 (d, J = 8.2 Hz, 2 H, ArH), 7.23 (br. s, 1 H, *NH*CO), 5.00 [br. s, 1 H, *NH*CO(O)], 4.86 (s, 2 H, CH_2Ar), 3.54 (dd, J = 5, 10 Hz, 2 H, *CH*$_2$NHCO), 3.40 [dd, J = 5, 10 Hz, 2 H, *CH*$_2$NHCO(O)], 3.03 (s, 3 H, ON*CH*$_3$), 1.49 [s, 9 H, (*CH*$_3$)$_3$-C], 1.42 [s, 9 H, (*CH*$_3$)$_3$-C] ppm. ^{13}C NMR (75 MHz, $CDCl_3$): δ = 167.3, 156.9, 139.1, 134.1, 129.1, 127.1, 81.4, 80.0, 75.8, 42.2, 39.9, 37.0, 28.3, 28.2 ppm. HR-MS (ESI): calcd. for $C_{21}H_{33}N_3O_6$ [M + Na]$^+$, 446.2262; found 446.2283.

***N*-(2-Boc-Aminoethyl)-4-[(*N*-Boc-*N*-benzylaminooxy)methyl]benzamide [Boc(B-AMB)]:** *tert*-Butyl 2-[4-(bromomethyl)phenylamido]-ethylcarbamate (160 mg, 0.45 mmol) and *tert*-butyl hydroxy(benzyl)carbamate (120 mg, 0.52 mmol) were treated as described for compound **Boc(B-AE)**. The crude product was absorbed on celite and purified with vacuum-column chromatography (EtOAc 0 to 50% in heptane) gave the pure product **Boc(B-AMB)** as colorless amorphous solid (197 mg, 90%). ^{1}H NMR (300 MHz, $CDCl_3$): δ = 7.75 (d, J = 8.2 Hz, 2 H, ArH), 7.30 (m, 7 H), 7.19 (br. s, 1 H, *NH*CO), 4.98 [br. s, 1 H, *NH*CO(O)], 4.71 (s, 2 H, CH_2Ar), 4.54 (s, 2 H, CH_2Ar), 3.53 (dd, J = 5, 10 Hz, 2 H, *CH*$_2$NHCO), 3.40 [dd, J = 5, 10 Hz, 2 H, *CH*$_2$NHCO(O)], 1.49 [s, 9 H, (*CH*$_3$)$_3$-C], 1.42 [s, 9 H, (*CH*$_3$)$_3$-C] ppm. ^{13}C NMR (75 MHz, $CDCl_3$): δ = 167.3, 156.6, 138.9, 136.7, 134.0, 129.2, 128.6, 128.4, 127.5, 127.0, 81.7, 80.0, 76.6, 54.1, 42.2, 39.9, 28.3, 28.2 ppm. HR-MS (ESI): calcd. for $C_{27}H_{37}N_3O_6$ [M + H]$^+$, 500.2755; found 500.2761.

2-(Benzylaminooxy)ethanamine Hydrochloride (B-AE): *N*-Benzyl-*O*-2-aminoethylhydroxylamine (135 mg, 0.37 mmol) was placed in a reaction vial and dissolved in HCl 4 M in dioxane (4 mL) whereupon a white crystalline precipitate quickly appeared. After 1 h stirring at room temp. the heterogeneous reaction mixture was diluted with diethyl ether and the precipitate was separated from the supernatant by centrifugation. The precipitate was washed with fresh ethyl ether (2 × 20 mL) and then dried under an air stream at first and finally under reduced pressure to yield the desired product **B-AE** (102 mg, 93%) as a white brittle solid. ^{1}H NMR (300 MHz, D_2O): δ = 7.51 (s, 5 H), 4.47 (s, 2 H, CH_2Ar), 3.53 (t, J = 5 Hz, 2 H, *CH*$_2$ON), 3.31 (t, J = 5, 10 Hz, 2 H, *CH*$_2$N) ppm. ^{13}C NMR (75 MHz, D_2O): δ = 130.2, 129.6, 129.1, 69.6, 53.8, 37.8 ppm. HR-MS (ESI): calcd. for $C_9H_{14}N_2O$ [M + H]$^+$, 167.1179; found 167.1180.

***N*-(2-Boc-Aminoethyl)-4-(aminooxymethyl)benzamide [Boc(AMB)]:** *tert*-Butyl 2-{4-[(1,3-dioxoisoindolin-2-yloxy)methyl]phenylamido}ethyl carbamate (205 mg, 0.57 mmol) was placed in a microwave vial and covered with a 1:1 mixture of DCM and acetonitrile (10 mL) whereupon hydrazine hydrate (430 μL, 8.54 mmol) was added. The vial was sealed, placed in the microwave cavity and irradiated at 65 °C for 15 min; after irradiation a white glossy precipitate was formed. The reaction mixture was filtered by suction on a pad of Celite with the aid of fresh acetonitrile (10 mL). The filtrate was concentrated in vacuo yielding the pure product **Boc(AMB)** as white solid (180 mg, 98%). ^{1}H NMR (300 MHz, $CDCl_3$): δ = 7.81 (d, J = 8.2 Hz, 2 H, ArH), 7.40 (d, J = 8.2 Hz, 2 H, ArH), 7.21 (br. s, 1 H, *NH*CO), 5.45 (br. s, 2 H, *NH*$_2$), 5.02 [br. s, 1 H, *NH*CO(O)], 4.72 (s, 2 H, CH_2Ar), 3.54 (m, 2 H, *CH*$_2$NHCO), 3.41 [m, 2 H, *CH*$_2$NHCO(O)], 1.42 [s, 9 H, (*CH*$_3$)$_3$-C] ppm. ^{13}C NMR (75 MHz, $CDCl_3$): δ = 167.4, 141.1, 133.6, 128.1, 127.1, 80.0, 77.2, 42.1, 39.9, 28.3 ppm. HR-MS (ESI): calcd. for $C_{15}H_{23}N_3O_4$ [M + Na]$^+$, 332.1581; found 332.1555.

***N*-(2-Aminoethyl)-4-(aminooxymethyl)benzamide Hydrochloride (AMB):** *tert*-Butyl 2-[4-(aminooxymethyl)phenylamido]ethyl carbamate (50 mg, 0.12 mmol) was deprotected as described for **B-AE**, giving the desired product **AMB** (33 mg, 99%) as a white powder. ^{1}H NMR (300 MHz, D_2O): δ = 7.85 (d, J = 8.4 Hz, 2 H, ArH), 7.60 (d, J = 8.4 Hz, 2 H, ArH), 5.15 (s, 2 H, CH_2Ar), 3.72 (t, J = 6 Hz, 2 H, C*H*$_2$NHCO), 3.27 (t, J = 6 Hz, 2 H, CH_2N) ppm. ^{13}C NMR (75 MHz, D_2O): δ = 170.9, 136.8, 134.1, 129.4, 127.7, 76.1, 39.3, 37.3 ppm. HR-MS (ESI): calcd. for $C_{10}H_{15}N_3O_2$ [M + H]$^+$, 210.1237; found 210.1250.

***N*-(2-Aminoethyl)-4-[(methylaminooxy)methyl]benzamide Hydrochloride [M-AMB]:** Compound **Boc(M-AMB)** was deprotected as described for compound **B-AE**, giving the desired product **M-AMB** (66 mg, 83%) as a white powder. ^{1}H NMR (300 MHz, D_2O): δ = 7.85 (d, J = 8.5 Hz, 2 H, ArH), 7.60 (d, J = 8.5 Hz, 2 H, ArH), 5.20 (s, 2 H, CH_2Ar), 3.72 (t, J = 6 Hz, 2 H, C*H*$_2$NHCO), 3.27 (t,

J = 6 Hz, 2 H, CH_2N), 3.04 (s, 3 H) ppm. ^{13}C NMR (75 MHz, D_2O): δ = 170.9, 136.6, 134.1, 129.4, 127.8, 75.1, 39.3, 37.3, 35.3 ppm. HR-MS (ESI): calcd. for $C_{11}H_{17}N_3O_2$ $[M + H]^+$, 224.1394; found 224.1404.

***N*-(2-Aminoethyl)-4-[(benzylaminooxy)methyl]Benzamide Hydrochloride [B-AMB]:** Compound **Boc(B-AMB)** was deprotected as described for compound **B-AE**, giving the desired product **B-AMB** (113 mg, 94%) as a white powder. ^1H NMR (300 MHz, D_2O): δ = 7.79 (d, J = 8.5 Hz, 2 H, ArH), 7.49–7.46 (m, 7 H), 5.12 (s, 2 H, CH_2Ar), 4.50 (s, 2 H, CH_2Ar), 3.70 (t, J = 6 Hz, 2 H, CH_2NHCO), 3.25 (t, J = 6 Hz, 2 H, CH_2N) ppm. ^{13}C NMR (75 MHz, D_2O): δ = 170.9, 136.9, 133.9, 130.5, 129.8, 129.2, 129.0, 128.8, 127.6, 75.3, 53.5, 39.2, 37.3 ppm. HR-MS (ESI): calcd. for $C_{17}H_{21}N_3O_2$ $[M + H]^+$, 300.1707; found 300.1711.

***N*-[*N*-Methyl-*O*-(benzamidoethyl)hydroxylamino] β-D-Glucopyranoside [Bz(M-AE)Glc]:** The aminooxy linker **M-AE** (24 mg, 0.15 mmol) and glucose (30 mg, 0.17 mmol) were placed in a reaction vial provided with stirrer and dissolved in a 5:1 mixture of methanol and acetic acid (5 mL), whereupon the vial was sealed and stirred at room temp. for 72 h. The reaction mixture was then reduced to dryness in vacuo and the residue taken up in pyridine (4 mL) and *N*-(benzoyloxy)succinimide (49 mg, 0.225 mmol) was added, then the resulting reaction mixture stirred at room temp. After 24 h the acetic anhydride (0.8 mL) was added and stirring was continued for a further 12 h at room temp. The volatiles were removed under vacuum and the residue taken up in DCM (10 mL) and extracted with saturated $NaHCO_3$ (1 × 20 mL) and brine. Purification with vacuum-column chromatography (EtOAc 0 to 100% in heptane, then methanol 0 to 5% in EtOAc) of the reaction crude after treatment with acetic anhydride gave a single peracetylated glucose conjugate, as characterized by HPLC-MS [eluent condition 2, 5 to 50% of D. MS (ESI): calcd. for $C_{24}H_{32}N_2O_{11}$ $(M + H)^+$, 525.2; found 525.1]. The intermediate product was then dissolved in methanol (2 mL) in an oven-dried reaction vial and treated with NaOMe 0.1 M in methanol (0.2 mL). The reaction mixture was stirred at room temp. for 12 h whereupon Amberlite-IR 120 was added to neutral pH. The solids were filtered off and the volatiles removed in vacuo yielding the pure glucose conjugate **Bz(M-AE)-Glc** (11 mg, 21%) as a white solid. ^1H NMR (300 MHz, D_2O): δ = 7.78 (dt, J = 7.0, 1.5 Hz, 2 H, ArH *ortho*), 7.64 (tt, J = 7.0, 1.5 Hz, 1 H, ArH *para*), 7.54 (tt, J = 7.0, 1.5 Hz, 2 H, ArH *meta*), 4.15 (d, J = 9.1 Hz, 1 H, 1-H), 4.0 (t, J = 5.4 Hz, 2H: CH_2NO), 3.91 (dd, J = 12.3, 2.2 Hz, 1 H, 6a-H), 3.72 (dd, J = 12.3, 5.3 Hz, 1 H, 6b-H), 3.63 (t, J = 5.4 Hz, 2 H, CH_2NHCO), 3.55–3.46 (m, 2 H, 2-H, 3-H), 3.40–3.30 (m, 2 H, 4-H, 5-H), 2.77 (s, 3 H, NCH_3) ppm. ^{13}C NMR (75 MHz, D_2O): δ = 171.0, 133.5, 132.1, 128.8, 127.0, 93.2, 77.4, 77.0, 70.9, 69.9, 69.4, 60.8, 38.9, 38.5 ppm. HR-MS (ESI): Calcd. for $C_{16}H_{24}N_2O_7$ $[M + Na]^+$, 379.1481; found 379.1486.

***N*-[*N*-Benzyl-*O*-(Acetamidoethyl)hydroxylamino] β-D Glucopyranoside, Ac(B-AE)Glc:** The aminooxy linker **B-AE** (40 mg, 0.17 mmol) and glucose (153 mg, 0.85 mmol) were placed in a reaction vial provided with stirrer and dissolved in a 5:1 mixture of methanol and acetic acid (5 mL), whereupon the vial was sealed and allowed to stir at room temp. for 72 h. The reaction mixture was then reduced to dryness in vacuo and the residue taken up in pyridine (4 mL) and treated with acetic anhydride (1 mL). The vial was sealed and the reaction stirred at room temp. for 24 h. The solvents were removed and the residue azeotroped several times in toluene in order to thoroughly remove pyridine. Purification with vacuum-column chromatography (EtOAc 0 to 100% in heptane) of the reaction crude after treatment with acetic anhydride gave a single peracetylated glucose conjugate, as characterized by HPLC-MS [eluent condition 1, 5 to 100% of B. MS (ESI): calcd. for $C_{25}H_{34}N_2O_{11}$ $(M + H)^+$, 539.2; found 539.2]. The intermediate product was then dissolved in methanol (3 mL) in an oven-dried reaction vial and treated with NaOMe 0.1 M in methanol (0.3 mL). The reaction mixture was stirred at room temp. for 12 h, whereupon Amberlite-IR 120 was added to neutral pH. The solids were filtered off and the volatiles removed in vacuo yielding the pure product **Ac(B-AE)-Glc** (37 mg, 59%) as a white solid. ^1H NMR (300 MHz, D_2O): δ = 7.49–7.38 (m, 5 H, ArH), 4.22 (d, J = 13.0 Hz, 1 H, $ArCH_{2a}N$), 4.16 (d, J = 9.0 Hz, 1 H, 1-H), 4.06 (d, J = 13.0 Hz, 1 H, $ArCH_{2b}N$), 3.96 (dd, J = 12.3, 2.0 Hz, 1 H, 6a-H), 3.75 (dd, J = 12.3, 5.3 Hz, 1 H, 6b-H), 3.70 (t, J = 5.0 Hz, 1 H, CH_2NO), 3.60 (t, J = 9.0 Hz, 1 H, 2-H), 3.57 (t, J = 5.0 Hz, 1 H, CH_2NO), 3.47 (t, J = 9.0 Hz, 1 H, 3-H), 3.43 (t, J = 9.0 Hz, 1 H, 4-H), 3.38–35 (m, 1 H, 5-H, from COSY), 3.16 (t, J = 5.4 Hz, 2 H, CH_2NHCO), 1.92 (s, 3 H, $NHCOCH_3$) ppm. ^{13}C NMR (75 MHz, D_2O): δ = 174.4, 137.0, 130.7, 129.1, 128.5, 92.2, 78.1, 77.8, 72.9, 70.4, 70.0, 61.5, 57.2, 38.9, 22.5 ppm. HR-MS (ESI): Calcd. for $C_{17}H_{26}N_2O_7$ $[M + Na]^+$, 393.1638; found 393.1649.

D-Glucose *O*-{4-[(2-Boc-Aminoethyl)aminocarbonyl]benzyl}oxime [Boc(AMB)Glc]: The aminooxy linker **AMB** (100 mg, 0.32 mmol) was treated with glucose in the same two-step procedure as described for **Ac(B-AE)Glc**. Purification with vacuum-column chromatography (EtOAc 0 to 100% in heptane, then methanol 0 to 5% in EtOAc) of the reaction crude after treatment with acetic anhydride gave a mixture of open- (major) and closed-ring (minor) peracetylated glucose conjugates, as characterized by HPLC-MS [eluent condition 1, 5 to 100% of B. MS (ESI): calcd. for the closed-ring form $C_{29}H_{41}N_3O_{13}$ $(M + H)^+$, 640.3; found 640.2; Calcd. for open-ring form $C_{31}H_{43}N_3O_{14}$ $(M + H)^+$, 682.3; found 682.2]. Following deacetylation, the pure product **Boc(AMB)Glc** (112 mg, 74%, isomeric mixture) was obtained as a white solid. ^1H NMR (300 MHz, D_2O): δ = 7.79–7.70 (m, 2 H, ArH), 7.57 (d, J = 6.7 Hz, 0.6 H, *E*-oxime 1-H), 7.52–7.44 (m, 2 H, ArH), 6.85 (d, J = 6.1 Hz, 0.2 H, *Z*-oxime 1-H), 5.16 (s, 0.4 H, OCH_2Ar *Z*-oxime) 5.14 (s, 1.2 H, OCH_2Ar *E*-oxime), 4.96 (t, J = 6.1 Hz, 0.2 H, *Z*-oxime 2-H), 4.88 (d, J = 9.0 Hz, 0.2 H, $OCH_{2a}Ar$), 4.84 (d, J = 9.0 Hz, 0.2 H, $OCH_{2b}Ar$, partly under H_2O signal), 4.33 (t, J = 6.9 Hz, 0.6 H, *E*-oxime 2-H), 4.23 (d, J = 9.0 Hz, 0.2 H, β-pyranose 1-H), 3.96–3.23 (m, 9.3 H), 1.32 [s, 9 H, $(CH_3)_3$-C] ppm. ^{13}C NMR (75 MHz, D_2O): δ = 170.5, 158.2, 153.0, 152.1, 141.1, 133.2, 128.7, 128.2, 127.3, 95.8, 90.2, 80.8, 77.1, 76.8, 76.7, 76.0, 75.9, 75.7, 75.1, 74.8, 74.1, 71.4, 71.4, 71.0, 70.8, 70.8, 70.2, 70.1, 69.9, 69.5, 69.3, 66.4, 63.0, 62.7, 60.7, 46.6, 39.8, 39.3, 37.3, 27.5 ppm. HR-MS (ESI): Calcd. for $C_{21}H_{33}N_3O_9$ $[M + Na]^+$, 494.2114; found 494.2118.

***N*-(*N*-Methyl-*O*-{4-[(2-acetamidoethyl)aminocarbonyl]benzyl}-*N*-hydroxylamino) β-D-Glucopyranoside [Ac(M-AMB)Glc]:** The aminooxy linker **M-AMB** (30 mg, 0.09 mmol) was treated with glucose in the same two-step procedure as described for **Ac(B-AE)Glc**. Purification with vacuum-column chromatography (MeOH 0 to 20% in EtOAc) of the reaction crude after treatment with acetic anhydride gave a single peracetylated glucose conjugate, as characterized by HPLC-MS (eluent condition 1, 5 to 100% of B). MS (ESI): Calcd. $C_{27}H_{37}N_3O_{12}$ $[M + H]^+$, 596.2; found 596.2. Following deacetylation, the pure product **Ac-MAMB-Glc** (14 mg, 49%) was obtained as a white solid. ^1H NMR (300 MHz, D_2O): δ = 7.75 (d, J = 8.4 Hz, 2 H, ArH), 7.55 (d, J = 8.4 Hz, 2 H, ArH), 4.88 (d, J = 10.8 Hz, 1 H, $OCH_{2a}Ar$), 4.84 (d, J = 10.8 Hz, 1 H, $OCH_{2b}Ar$), 4.16 (d, J = 9.0 Hz, 1 H, 1-H), 3.91 (dd, J = 12.3, 2.0 Hz, 1 H, 6a-H), 3.74 (dd, J = 12.3, 5.0 Hz, 1 H, 6b-H), 3.58 (t, J = 9.0 Hz, 1 H, 2-H), 3.55–3.50 (m, 3 H), 3.47–3.37 (m, 4 H), 2.80 (s, 3 H, NCH_3), 1.99 ($NCOCH_3$) ppm. ^{13}C NMR (75 MHz, D_2O): δ = 174.4, 170.7, 139.9, 133.6, 129.4, 127.2, 93.2, 77.2, 77.0, 74.5, 69.9,

69.4, 60.7, 39.2, 38.7, 38.7, 21.8 ppm. HR-MS (ESI): Calcd. for $C_{19}H_{29}N_3O_8$ [M + Na]$^+$, 450.1852; found 450.1832.

***N*-(*N*-Benzyl-*O*-{4-[(2-acetamidoethyl)aminocarbonyl]benzyl}-hydroxylamino) β-D-Glucopyranoside [Ac-BAMB-Glc]:** The aminooxy linker **B-AMB** (35 mg, 0.095 mmol) was treated with glucose in the same two-step procedure as described for **Ac(B-AE)Glc**. Purification with vacuum-column chromatography (MeOH 0 to 40% in EtOAc) of the reaction crude after treatment with acetic anhydride gave a single glucose conjugate, as characterized by HPLC-MS (eluent condition 1, 5 to 100% of B). MS (ESI): calcd. $C_{33}H_{41}N_3O_{12}$ [M + H]$^+$, 672.3; found 672.2.2. Following deacetylation, the pure product **Ac-BAMB-Glc** (16 mg, 35%) was obtained as a white solid. ^{1}H NMR (300 MHz, D_2O): δ = 7.55 (d, J = 8.3 Hz, 2 H, ArH), 7.47–7.39 (m, 5 H, ArH), 7.28 (d, J = 8.3 Hz, 2 H, ArH), 4.64 (d, J = 10.3 Hz, 1 H, OCH_{2a}Ar), 4.47 (d, J = 10.3 Hz, 1 H, OCH_{2b}Ar), 4.22 (d, J = 12.8 Hz, 1 H, NCH_{2a}Ar), 4.18 (d, J = 9.0 Hz, 1 H, 1-H), 4.08 (d, J = 10.3 Hz, 1 H, NCH_{2b}Ar), 3.93 (dd, J = 12.3, 2.0 Hz, 1 H, 6a-H), 3.76 (dd, J = 12.3, 5.0 Hz, 1 H, 6b-H), 3.69 (t, J = 9.0 Hz, 1 H, 2-H), 3.52–3.46 (m, 3 H), 3.43–3.37 (m, 4 H), 1.98 (s, 3 H, NCOCH_3) ppm. ^{13}C NMR (75 MHz, D_2O): δ = 174.4, 170.7, 139.4, 136.3, 133.6, 130.2, 129.6, 128.5, 127.9, 127.1, 91.6, 77.2, 77.2, 76.0, 70.0, 69.4, 60.8, 56.8, 39.2, 38.7, 21.8 ppm. HR-MS (ESI): Calcd. for $C_{25}H_{33}N_3O_8$ [M + Na]$^+$, 526.2165; found 526.2196.

Hydrolytic Stability of Glucose-Linker Conjugates: Stock solutions of each glucose conjugate (20 mM in DMSO) were prepared and 50 μL of these were diluted to 1 mL with each of the relevant buffer solutions (50 mM, sodium phosphate pH 3; sodium acetate pH 4 and 5) in order to obtain 1 mM final concentration of conjugate (time of dilution set to be t_0 of the hydrolysis reaction course). The solutions were incubated at room temp. inside the HPLC autosampler in the dark and injected into HPLC at intervals during 4 d. All hydrolysis were monitored with either Phenomenex Hydro 150 × 3.0 mm, 3 Å or Dionex Acclaim 150 × 5 mm, 5 Å columns with flow rate 1.0 mL/min and linear gradient flow of B 5 to 50% in A over 15 min (A = NH_4OAc 10 mM, pH 5.8; B = 9:1 *v*/*v* MeCN/NH_4OAc 100 mM pH 5.8). Peaks area at 230 nm [except for **Ac(B-AE)Glc** where 215 nm was used instead] were used to estimate the conjugate/linker ratio, which is reported as fraction of conjugate remaining according to the formula [$A_{conjugate}/(A_{conjugate} + A_{linker})$] and plotted vs. time for each of the three buffer systems. The points thus collected fitted well an exponential decay function, which allowed calculating the pseudo first-order rate constant and half-lives of the conjugates.

General Preparation of Glycoconjugate Probes for Microarray Fabrication: Stock solutions (40 mM) of each of the free reducing glycans, stock solutions (120 mM) of linkers **M-AMB** and **B-AMB** and a 60 mM stock solution of linker **AMB** were prepared in 0.1 M NH_4OAc buffer, pH 4.5 (to the chitopentaose stock solution 20% DMSO was added for solubility). Aliquots from the relevant glycan and the linker stock solution were mixed 1:1 (v/v, typically 50 or 100 μL) in a tight seal Eppendorf tube and incubated at 37 °C under gentle shaking. At regular intervals the reaction mixtures were injected into HPLC (elution condition 2). After 24 to 72 h all the reactions reached equilibration and no more product formation was observed. The above procedure was implemented for the preparation of the batch of **(B-AMB)LacNAc** where 100 μL of reaction mixture contained 50 mM B-AMB (41.6 μL) and 1 mM *N*-acetyllactosamine (2.5 μL) and purified by extraction. **Purification procedure by HPLC**: 20 to 40 μL aliquots of the reaction mixtures at equilibration were injected directly into HPLC (elution condition 2) and the fractions containing the product (as assessed by UV chromatogram) were hand-collected and freeze-dried. When a conjugate was present in more than one isomer, no effort was done to separate them from one anther; hence the different isomers were pooled together. The freeze-dried pellets were taken up in print buffer (200 μL) and the conjugate concentration for each sample was estimated via calibration curves obtained with stock solutions of the relevant free linker. **Purification procedure by extraction**: reaction mixtures of *N*-acetyllactosamine and mannobiose conjugates of **B-AMB** were freeze-dried and the resulting pellets taken up with 0.1 M NH_4OAc buffer (200 μL), pH 9.0 in an Eppendorf vial. Then DCM (800 μL) was added to each vial and the resulting two-layer mixtures were vigorously shaken for 5 min. After centrifugation, the DCM layer was removed with a pipette. A total of 8 extraction cycles with DCM were performed, the last which was kept whilst stirring overnight. After the extraction series, the water layer was analyzed by HPLC-MS (elution condition 1), showing only negligible traces of free linker left. The extracted samples were freeze-dried and the resulting pellets taken up in print buffer (200 μL) and their concentrations estimated via a calibration curve as mentioned above. **(AMB)Lac**, HR-MS (ESI): calcd. for $C_{22}H_{35}N_3O_{12}$ [M + H]$^+$, 534.2294; found 534.2317; **(AMB)LacNAc**, HR-MS (ESI): calcd. for $C_{24}H_{38}N_4O_{12}$ [M + H]$^+$, 575.2559; found 575.2519; **(AMB)Man$_2$**, HR-MS (ESI): calcd. for $C_{22}H_{35}N_3O_{12}$ [M + Na]$^+$, 556.2113; found 556.2771; **(AMB)GlcNAc$_5$**, HR-MS (ESI): calcd. for $C_{50}H_{80}N_8O_{27}$ [M + H]$^+$, 1225.5206; found 1225.5292; **(M-AMB)Lac**, HR-MS (ESI): calcd. for $C_{23}H_{37}N_3O_{12}$ [M + H]$^+$, 548.2450; found 548.2480; **(M-AMB)LacNAc**, HR-MS (ESI): calcd. for $C_{25}H_{40}N_4O_{12}$ [M + H]$^+$, 589.2715; found 589.2720; **(M-AMB)Man$_2$**, HR-MS (ESI): calcd. for $C_{23}H_{37}N_3O_{12}$ [M + H]$^+$, 548.2450; found 548.2447; **(B-AMB)Lac**, HR-MS (ESI): calcd. for $C_{29}H_{41}N_3O_{12}$ [M + H]$^+$, 624.2763; found 624.2778; **(B-AMB)-LacNAc**, HR-MS (ESI): calcd. for $C_{31}H_{44}N4O_{12}$ [M + H]$^+$, 665.3028; HPLC purified; found 665.3032; extraction purified; found 665.3041; **(B-AMB)Man$_2$**, HR-MS (ESI): calcd. for $C_{29}H_{41}N_3O_{12}$ [M + H]$^+$, 624.2763; HPLC purifed; found 624.2732; extraction purified; found 624.2741.

Printing of Arrays: The glycan arrays were fabricated by robotic contact printing of approx. 6 nL of glycan-linker conjugates in print buffer (150 mM phosphare, 0.005% tween-20, pH 8.5) onto NHS-activated glass slide (Nexterion Slide H, Schott AG, Mainz, Germany). The conjugates were distributed in 384-well source plates (20 μL per well) and structure was printed in 4 different concentrations in fivefold dilutions (250–2 μM) and each dilution deposited 4 times, thus creating a 4 × 4 subgrid with a 0.21 mm pitch between spots for each conjugate. The needles dwell time in the wells was of 4 seconds and the pins underwent 3 wash cycles in between visits. The complete array pattern was printed in 16 replicas, distributed in two columns and 8 rows. Immediately after printing the slides were incubated at 80% humidity for 60 min. The NHS groups in the unprinted areas of the slides were blocked by immersion in the blocking buffer (50 mM ethanolamine in 50 mM borate buffer, pH 9.2) for 1 h. Slides were rinsed in Millipore water, dried by centrifuging and probed. The slide that were not to be probed immediately were stored at –18 °C before the blocking step.

On-Slide Hydrolysis of Glucose-Linker Conjugates: A printed and blocked slide was equipped with the 16-well superstructure in order to create incubation wells for each of the 16 replica subarrays present on a slide. Nine wells were filled with 90 μL of phosphate buffer 50 mM, pH 3 each and the remaining wells filled with print buffer, whereupon an adhesive cover tape was applied over the whole slide. After 6 h the eight wells holding pH 3 solution were emptied and backfilled with print buffer. After 24 h all wells were emptied and backfilled with print buffer. Finally, after 36 h all wells were emp-

tied and the slide washed by immersion in PBST (phosphate-buffered saline, 0.05% Tween-20), PBS and Millipore water whereupon lectin staining with RCA I (10 μg/mL) followed as described below.

Lectin Staining: Blocked glycan-linker microarrays not coming from the hydrolysis study were equipped with the 16-well superstructure and immersed in PBS for 5 min. Incubation followed a two-step procedure, in which at first solutions of biotin-tagged lectins RCA I, ConA, ECA and WGA in PBST (all applied at 10 μg/mL, 90 μL per well) were placed in the relevant wells. Then Alexa Fluor 488-conjugate streptavidin in PBST (0.4 μg/mL, 90 μL per well) was placed in all wells for detection. The slides were incubated for 1 h at 80% humidity for each incubation step. In between incubations the slides were washed by immersing them 2 min in each *i*) PBST, *ii*) PBS, and *iii*) Millipore water. Finally, the superstructure was removed; the slides rinsed with Millipore water and dried by centrifuge. Laser scanner imaging was immediately undertaken.

Supporting Information (see also the footnote on the first page of this article): Plots of the hydrolysis of all glucose-linker conjugates over time, representative chromatograms and UV-spectra utilized for monitoring the hydrolysis of glucose-linker conjugates, experimental procedure for **Ac(B-AMB)GlcNAc**, HPLC-MS of peracetylated B-AMB-Mannose conjugate, ^{1}H and ^{13}C NMR spectra of all new compounds, COSY NMR spectra of **Ac(B-AE)Glc**, **Ac-(B-AMB)Glc** and **Ac(B-AMB)GlcNAc**, HSQC NMR spectra of **Ac-(B-AE)Glc** and **Ac(B-AMB)Glc**.

Acknowledgments

We thank Dr. Mikkel B. Thygesen for valuable discussions and Stig Jacobsen for acquiring mass spectra. Support from the Danish Council for Technology and Innovation as well as the Danish National Research Foundation (grants to K. J. J.) is gratefully acknowledged.

[1] R. Apweiler, H. Hermjakob, N. Sharon, *Biochim. Biophys. Acta* **1999**, *1473*, 4–8.
[2] M. Fukuda, *Biochim. Biophys. Acta* **2002**, *1573*, 394–405.
[3] A. E. Smith, A. Helenius, *Science* **2004**, *304*, 237–242.
[4] A. Varki, M. J. Chrispeels, *Glycobiology* **1993**, *3*, 97–130.
[5] J. G. Velasquez, S. Canovas, P. Barajas, J. Marcos, M. Jimenez-Movilla, R. Gutiérrez Gallego, J. Ballesta, M. Aviles, P. Coy, *Mol. Reprod. Dev.* **2007**, *74*, 617–628.
[6] M. M. Fuster, J. D. Esko, *Nat. Rev. Cancer* **2005**, *5*, 526–542.
[7] A. Varki, N. Sharon, in: *Essentials in Glycobiology*, 2nd edition (Eds.: A. Varki, R. Cummings, J. D. Esko, H. Freeze, G. Hart, J. Marth), Cold Spring Harbor Laboratory Press, Plainview, NY, **2008**, pp. 1–22.
[8] K. Larsen, M. Thygesen, F. Guillaumie, W. Willats, K. J. Jensen, *Carbohydr. Res.* **2006**, *341*, 1209–1234.
[9] a) J. C. Paulson, O. Blixt, B. E. Collins, *Nat. Chem. Biol.* **2006**, *2*, 238–248; b) P.-H. Liang, C.-Y. Wu, W. A. Greenberg, C.-H. Wong, *Curr. Opin. Chem. Biol.* **2008**, *12*, 86–92.
[10] a) S. Park, M.-R. Lee, I. Shin, *Chem. Commun.* **2008**, *37*, 4389; b) T. Horlacher, P. H. Seeberger, *Chem. Soc. Rev.* **2008**, *37*, 1414–1422; c) N. Laurent, J. Voglmeir, S. L. Flitsch, *Chem. Commun.* **2008**, *37*, 4400–4412.
[11] M. Mammen, S. Choi, G. Whitesides, *Angew. Chem. Int. Ed.* **1998**, *37*, 2754–2794.
[12] M. C. Bryan, F. Fazio, H.-K. Lee, C.-Y. Huang, A. Chang, M. D. Best, D. A. C. O. Blixt, J. C. Paulson, D. Burton, I. A. Wilson, C.-H. Wong, *J. Am. Chem. Soc.* **2004**, *126*, 8640–8641.
[13] a) O. Blixt, S. Head, T. Mondala, C. Scanlan, M. E. Huflejt, R. Alvarez, M. C. Bryan, F. Fazio, D. Calarese, J. Stevens, N. Razi, D. J. Stevens, J. J. Skehel, I. van Die, D. R. Burton, I. A. Wilson, R. Cummings, N. Bovin, C.-H. Wong, J. C. Paulson, *Proc. Natl. Acad. Sci. USA* **2004**, *101*, 17033–17038; b) J. L. De Paz, C. Noti, P. H. Seeberger, *J. Am. Chem. Soc.* **2006**, *128*, 2766–2767.
[14] M.-R. Lee, I. Shin, *Angew. Chem. Int. Ed.* **2005**, *44*, 2881–2884.
[15] a) S. J. Park, I. Shin, *Angew. Chem. Int. Ed.* **2002**, *41*, 3180–3182; b) B. Houseman, E. Gawalt, M. Mrksich, *Langmuir* **2003**, *19*, 1522–1531.
[16] M. Köhn, R. Wacker, C. Peters, H. Schröder, L. Soulère, R. Breinbauer, C. M. Niemeyer, H. Waldmann, *Angew. Chem. Int. Ed.* **2003**, *42*, 5830–5834.
[17] a) S. E. Cervigni, P. Dumy, M. Mutter, *Angew. Chem. Int. Ed. Engl.* **1996**, *35*, 1230–1232; b) Y. Hatanaka, U. Kempin, J.-J. Park, *J. Org. Chem.* **2000**, *65*, 5639–5643; c) B. L. Ridley, M. D. Spiro, J. Glushka, P. Albersheim, A. Darvill, D. Mohnen, *Anal. Biochem.* **1997**, *249*, 10–19; d) N. S. Flinn, M. Quibell, T. P. Monk, M. K. Ramjee, C. J. Urch, *Bioconjugate Chem.* **2005**, *16*, 722–728; e) F. Guillaumie, O. R. T. Thomas, K. J. Jensen, *Bioconjugate Chem.* **2002**, *13*, 285–294.
[18] a) Y. Liu, T. Feizi, M. Campanerorhodes, R. Childs, Y. Zhang, B. Mulloy, P. Evans, H. Osborn, D. Otto, P. Crocker, *Chem. Biol.* **2007**, *14*, 847–859; b) G. Chen, N. Pohl, *Org. Lett.* **2008**, *10*, 785–788.
[19] M.-R. Lee, I. Shin, *Org. Lett.* **2005**, *7*, 4269–4272.
[20] Z.-l. Zhi, A. K. Powell, J. E. Turnbull, *Anal. Chem.* **2006**, *78*, 4786–4793.
[21] B. Xia, Z. S. Kawar, T. Ju, R. A. Alvarez, G. P. Sachdev, R. D. Cummings, *Nat. Methods* **2005**, *11*, 845–850.
[22] a) J. Kalia, R. T. Raines, *Angew. Chem. Int. Ed.* **2008**, *47*, 7523–7526; b) A. Dirksen, S. Dirksen, T. M. Hackeng, P. E. Dawson, *J. Am. Chem. Soc.* **2006**, *128*, 15602–15603.
[23] F. Peri, P. Dumy, M. Mutter, *Tetrahedron* **1998**, *54*, 12269–12278.
[24] M. B. Thygesen, J. Sauer, K. J. Jensen, *Chem. Eur. J.* **2009**, *15*, 1649–1660.
[25] O. Bohorov, H. Andersson-Sand, J. Hoffmann, O. Blixt, *Glycobiology* **2006**, *16*, 21C–27C.
[26] J. Wang, M. Uttamchandani, J. Li, Mi. Hu, S. Q. Yao, *Chem. Commun.* **2006**, *36*, 3783–3785.
[27] S. Buchini, A. Buschiazzo, S. G. Withers, *Angew. Chem. Int. Ed.* **2008**, *47*, 2700–2703.
[28] P. Finch, Z. J. Merchant, *J. Chem. Soc. Perkin Trans. 1* **1975**, 1682–1686.
[29] a) M. R. Carrasco, M. J. Nguyen, D. R. Burnell, M. D. MacLaren, S. M. Hengel, *Tetrahedron Lett.* **2002**, *43*, 5727–5729; b) M. R. Carrasco, R. T. Brown, *J. Org. Chem.* **2003**, *68*, 8853–8858; c) J. Langenhan, B. Griffith, J. Thorson, *J. Nat. Prod.* **2005**, *68*, 1696–1711; d) N. Matsubara, K. Oiwa, T. Hohsaka, R. Sadamoto, K. Niikura, N. Fukuhara, A. Takimoto, H. Kondo, S.-I. Nishimura, *Chem. Eur. J.* **2005**, *11*, 6974–6981.
[30] J. M. Langenhan, N. R. Peters, I. A. Guzei, F. M. Hoffmann, J. S. Thorson, *Proc. Natl. Acad. Sci. USA* **2005**, *102*, 12305–12310.
[31] A. V. Gudmundsdottir, C. E. Paul, M. Nitz, *Carbohydr. Res.* **2009**, *344*, 278–284.
[32] J. Haas, R. Kadunce, *J. Am. Chem. Soc.* **1962**, *84*, 4910–4913.
[33] M. Vila-Perelló, R. Gutiérrez Gallego, D. Andreu, *ChemBioChem* **2005**, *6*, 1831–1838.
[34] H. Bittiger, H. P. Schnebli, *Concanavaline A as a Tool*, John Wiley & Sons, **1976**.
[35] A. M. Wu, J. H. Wu, T. Singh, L. J. Lai, Z. Yang, A. Herp, *Mol. Immunol.* **2006**, *43*, 1700–1715.
[36] Y. Itakura, S. Nakamura-Tsuruta, J. Kominami, N. Sharon, K.-I. Kasai, J. Hirabayashi, *J. Biochem.* **2007**, *142*, 459–469.
[37] Y. Nagata, M. M. Burger, *J. Biol. Chem.* **1974**, *249*, 3116–3122.
[38] P.-H. Liang, S.-K. Wang, C.-H. Wong, *J. Am. Chem. Soc.* **2007**, *129*, 11177–11184.
[39] C. Jiménez-Castells, B. G. Torre, D. Andreu, R. Gutiérrez-Gallego, *Glycoconjugate J.* **2008**, *25*, 879–887.

[40] J. Brand, T. Huhn, U. Groth, J. C. Jochims, *Chem. Eur. J.* **2005**, *12*, 499–509.
[41] Peracetylation experiments of conjugate between **B-AMB** and mannose showed no presence of open-chain isomer with HPLC-ESI MS. See Supporting Information for details.
[42] S. Park, M.-R. Lee, I. Shin, *Bioconjugate Chem.* **2009**, *20*, 155–162.
[43] X. Song, B. Xia, S. Stowell, Y. Lasanajak, D. Smith, R. Cummings, *Chem. Biol.* **2009**, *16*, 36–47.
Received: October 29, 2009
Published Online: December 9, 2009

